

Pareto-Optimal Anytime Algorithms via Bayesian Racing

JONATHAN WURTH, Universität Augsburg, Germany

HELENA STEGHERR, Universität Augsburg, Germany

NEELE KEMPER, Universität Augsburg, Germany

MICHAEL HEIDER, Universität Augsburg, Germany

JÖRG HÄHNER, Universität Augsburg, Germany

Selecting an optimization algorithm requires comparing candidates across problem instances, but the computational budget for deployment is often unknown at benchmarking time. Current methods either collapse anytime performance into a scalar, require manual interpretation of plots, or produce conclusions that change when algorithms are added or removed. Moreover, methods based on raw objective values require normalization, which needs bounds or optima that are often unavailable and breaks coherent aggregation across instances. We propose a framework that formulates anytime algorithm comparison as Pareto optimization over time: an algorithm is non-dominated if no competitor beats it at every timepoint. By using rankings rather than objective values, our approach requires no bounds, no normalization, and aggregates coherently across arbitrary instance distributions without requiring known optima. We introduce PolarBear (Pareto-optimal anytime algorithms via Bayesian racing), a procedure that identifies the anytime Pareto set through adaptive sampling with calibrated uncertainty. Bayesian inference over a temporal Plackett-Luce ranking model provides posterior beliefs about pairwise dominance, enabling early elimination of confidently dominated algorithms. The output Pareto set together with the posterior supports downstream algorithm selection under arbitrary time preferences and risk profiles without additional experiments.

CCS Concepts: • **Computing methodologies** → **Ranking**; *Uncertainty quantification*; • **Theory of computation** → **Bayesian analysis**; *Active learning*; **Optimization with randomized search heuristics**.

Additional Key Words and Phrases: anytime optimization, algorithm benchmarking, Plackett-Luce, Bayesian experiment design, racing algorithms, algorithm selection

ACM Reference Format:

Jonathan Wurth, Helena Stegherr, Neele Kemper, Michael Heider, and Jörg Hähner. 2026. Pareto-Optimal Anytime Algorithms via Bayesian Racing. *ACM Trans. Evol. Learn. Optim.* 1, 1, Article 1 (February 2026), 38 pages. <https://doi.org/XXXXXXX.XXXXXXX>

1 Introduction

Selecting an optimization algorithm for deployment requires comparing candidates across problem instances of interest. However, the computational budget available for optimization is often unknown at benchmarking time. It may depend on available resources, user patience, or external constraints that only materialize at deployment time. When deployment arrives, budget information takes many forms: a fixed allocation (“at most 1000 evaluations”), a range (“between 1 and

Authors’ Contact Information: Jonathan Wurth, jonathan.wurth@uni-a.de, Universität Augsburg, Augsburg, Germany; Helena Stegherr, helena.stegherr@uni-a.de, Universität Augsburg, Augsburg, Germany; Neele Kemper, neele.kemper@uni-a.de, Universität Augsburg, Augsburg, Germany; Michael Heider, michael.heiderr@uni-a.de, Universität Augsburg, Augsburg, Germany; Jörg Hähner, joerg.haehner@uni-a.de, Universität Augsburg, Augsburg, Germany.

Permission to make digital or hard copies of all or part of this work for personal or classroom use is granted without fee provided that copies are not made or distributed for profit or commercial advantage and that copies bear this notice and the full citation on the first page. Copyrights for components of this work owned by others than the author(s) must be honored. Abstracting with credit is permitted. To copy otherwise, or republish, to post on servers or to redistribute to lists, requires prior specific permission and/or a fee. Request permissions from permissions@acm.org.

© 2026 Copyright held by the owner/author(s). Publication rights licensed to ACM.

ACM 2688-3007/2026/2-ART1

<https://doi.org/XXXXXXX.XXXXXXX>

2 hours”), a distribution reflecting resource uncertainty (“probably around 90 minutes, but possibly cut short”), or a preference weighting early versus late performance (“solutions found in the first minute matter most”). This raises a fundamental question: *what should we compute offline to support algorithm selection under any budget information that may arise at deployment time?* This question is naturally addressed by anytime algorithms, which can return a valid solution at any point during execution, with performance defined at every potential budget. For black-box optimization on noiseless problems, this property holds naturally, since we can track the best solution found so far. Analyzing anytime performance means evaluating not just at a fixed final budget, but throughout execution.

A powerful tool to analyze the anytime performance of stochastic optimization algorithms is the Empirical Attainment Function (EAF), which is the empirical estimate of the probability that an algorithm attains a solution with objective value of at least z by time t [López-Ibáñez et al. 2024]. A common summary of this is the EAF-based Empirical Cumulative Distribution Function (ECDF), which partially integrates the EAF using an interval of objective values by counting the proportion of the interval that is attained by the algorithm at each point in time. The lower bound of the interval is usually chosen as the best possible (or best known possible) attainable objective value, i.e., the global optimum. The EAF and EAF-based ECDF (hereafter simply ECDF) are commonly plotted and analyzed visually. For tasks involving automatic evaluation, such as automated algorithm configuration or design, the Area over the Convergence Curve (AOCC) has established itself as a popular measure [de Nobel et al. 2021; López-Ibáñez and Stützle 2014; van Stein et al. 2024; Ye et al. 2022]. It is, despite its name, most easily defined as the expected area *under* the ECDF, i.e., its integral over time.

While EAF and ECDF are sophisticated approaches for analyzing anytime performance across repeated executions and different algorithms on a single problem instance, aggregating across multiple instances comes with several problems. On a single instance, the interval of objective values to plot in the EAF or integrate in the ECDF can simply be derived from the observed data. However, this interval is instance-dependent, which means that it is not possible to combine or average the EAF and ECDF across instances without some form of normalization. In practice, this is addressed by min-max normalizing the objective values per instance-dependent interval and then aggregating across instances [López-Ibáñez et al. 2024]. We argue that this step of min-max normalization is not principled. Min-max normalization requires the interval bounds, typically the global optimum and a worst-case value. Firstly, for many problems, the global optimum is unknown or expensive to determine, limiting applicability to well-studied benchmark functions, or requiring to derive these bounds from observed data. In the latter case, adding a new algorithm that finds better or worse solutions shifts all normalizations, which means that historical comparisons become invalid, and results depend on which algorithms are included. Secondly, equal distances in normalized space usually do not correspond to equal difficulty. Improving from a normalized value of 0.9 to 0.5 may be trivial, while improving from 0.1 to 0.05 may require exponentially more effort. Averaging normalized values implicitly assumes uniform difficulty across the scale.

While AOCC inherits these same issues, it has one more fundamental limitation: it collapses anytime performance into a single scalar. While this makes it easy to use as a tuning objective, since it imposes a total order, it obscures the tradeoffs over time. An algorithm that converges quickly but stagnates becomes indistinguishable from one that starts slowly but continues improving, yet these represent different behaviors that users may value differently.

Additionally, conclusions about algorithm performance are inherently uncertain when experimental budgets are limited [Vermetten et al. 2022]. Running each algorithm on a handful of instances may suggest one is better, but how confident should we be? When have we gathered enough evidence to act? Traditional methods provide point estimates or p-values, neither of which

directly answers these questions. A Bayesian approach quantifies uncertainty as probability: we can ask “what is the probability that A is better than B under some preference over budgets, given what we have observed?” and receive a calibrated answer that updates as evidence accumulates.

These points motivate a framework for anytime performance evaluation that is (1) scale-free, (2) preserves tradeoffs over time, (3) quantifies its uncertainty, and (4) is fully automatable. This paper proposes a Bayesian framework for anytime algorithm comparison that satisfies these criteria. The central idea is to treat each budget or point in time as a separate objective, yielding a Pareto set of non-dominated algorithms over time. Using rankings rather than objective values enables coherent aggregation across arbitrary instances without normalization. We propose a racing procedure, called POLARBEAR, to efficiently identify this Pareto set with calibrated uncertainty by eliminating dominated algorithms early and terminating when pairwise relationships are resolved. The framework requires no prior knowledge about objective bounds or optima, preserves anytime tradeoffs, and provides fully automated evaluation. The output is a Pareto set over potential budgets together with a posterior that support downstream selection under arbitrary time preferences and risk profiles.

2 Scale-free Anytime Performance

We define an anytime algorithm A as a randomized procedure with access to an objective function $f : \mathcal{X} \rightarrow \mathcal{Y}$. For random seeds $\omega \in \Omega$, execution of $A(f, \omega)$ produces a trajectory $\mathbf{x}_A : \mathcal{T} \rightarrow \mathcal{X}$ mapping each timepoint $t \in \mathcal{T} \subset \mathbb{R}_{\geq 0}$ to a solution $x \in \mathcal{X}$. The performance trajectory is $\mathbf{g}_A : \mathcal{T} \rightarrow \mathcal{Y}, t \mapsto f(\mathbf{x}(t))$. Assuming minimization and noiseless f as well as a total order on \mathcal{Y} , the best-so-far trajectory $\mathbf{g}_A^*(t) = \min_{s \leq t} \mathbf{g}_A(s)$ can be computed externally by tracking all evaluated solutions. An algorithm thus induces a distribution over trajectories \mathbf{g}^* . Note that algorithms with budget-dependent components (e.g., adaptation based on the proportion of budget spent) define a family of anytime algorithms, one per configured budget b . Each member $A(b)$ has a well-defined trajectory and can be included as a separate algorithm.

Rather than modeling best-so-far trajectories $\mathbf{g}^*(t)$ directly, we observe only the induced rankings: given algorithms $\mathbf{A} = \{A_1, \dots, A_n\}$ evaluated on the same instance at the same timepoints, we record the order of $\mathbf{g}_{A_i}^*(t)$ at each time t . This is a deliberate reduction, motivated by the following observations.

Consider what we actually know when comparing algorithms. For example, we know that algorithm A found a solution with objective value 47.3 and algorithm B found one with value 52.1. We therefore know $A < B$, assuming minimization. But what does the difference of 4.8 mean? Is it meaningful? Is it harder to achieve than a difference of 4.8 elsewhere in the objective space? Answering these questions requires knowledge we typically do not have: the structure of the fitness landscape, the distribution of objective values, the relationship between objective differences and search difficulty. The ranking $A < B$ is a fact; the meaning of 4.8 is an interpretation that requires assumptions we cannot generally justify.

The standard solution to comparing across instances is min-max normalization: transform objective values to $[0, 1]$ via $\tilde{y} = (y - y_{\min}) / (y_{\max} - y_{\min})$, where y_{\min} and y_{\max} are instance-specific bounds. This makes values numerically comparable, but the comparability is superficial. Min-max normalization implicitly assumes that difficulty is uniform across the objective range. Under this assumption, improving from normalized value 0.9 to 0.8 represents the same algorithmic achievement as improving from 0.2 to 0.1. In practice, this is rarely true. On many landscapes, early progress is easy while the final approach to the optimum is hard; on others, escaping a local optimum is the key difficulty. The former intuition is usually encoded by applying a logarithmic transformation before normalization, so that values closer to y_{\min} receive increasingly greater weight,

i.e., progress near the optimum is harder and therefore more informative. The intuition may be reasonable, but the transformation is only coherent if y_{\min} is the true global optimum. When the global optimum is unknown and y_{\min} is derived from observed data, the log transformation amplifies the instability: a new algorithm that finds a better solution shifts y_{\min} , which compresses the entire previous range and drastically changes the relative importance of all prior observations.

We argue that the problem with normalization is not merely practical but fundamental. Any such procedure either requires information about the problem instances that is unavailable in black-box settings, or extracting this information is at least as hard as solving the instance itself (in the case of the global optimum, exactly as hard). Min-max normalization is therefore not an approximation to a correct procedure; it is an unprincipled default that happens to produce numbers in a standard range. The log transformation adds another layer of assumptions while amplifying sensitivity to data-derived bounds.

The optimization community has already recognized the problem of interpreting the scale of objective values through the design of modern algorithms. Many state-of-the-art metaheuristics, including CMA-ES and differential evolution, deliberately discard magnitude information during search. The motivation is invariance: algorithm behavior should not depend on monotonic transformations of the objective function [Hansen 2023]. This makes algorithms robust to poorly scaled objectives, objectives with outliers, and objectives where the relationship between value and difficulty is unknown. If invariance is the right principle for designing search algorithms, it should also be the right principle for evaluating them. An algorithm that is invariant to monotonic transformations of the objective should be evaluated by a method that is equally invariant.

Rankings require none of these assumptions. The statement that A beats B on a given instance is meaningful regardless of objective scale, landscape structure, or which other algorithms were included in the comparison. One might object that rankings discard potentially useful information. This is true, but only relevant if magnitude carries reliable information. When objective scale is meaningful, known, and comparable across instances, cardinal information can improve statistical efficiency. Such conditions sometimes hold in carefully constructed synthetic benchmarks with known optima and well-understood structure. But we argue that this is the exception rather than the rule (even the well-studied BBOB suite is notably not one such exception, i.e., “difficulty versus function value is not uniform” [Hansen et al. 2009]). The default situation in black-box optimization is that we know little about the objective function beyond what we observe during search. Rankings extract exactly the information we can trust, namely relative performance, without requiring assumptions about what objective differences mean. They are therefore not a compromise forced by missing information but the maximally robust choice given typical conditions.

Given that we observe rankings, we now ask: what is the appropriate model? Since observed trajectories are independent measurements per algorithm, our modeling process should reflect this property. Specifically, this means respecting the independence of irrelevant alternatives (IIA), i.e., the inclusion of an algorithm C should not change our belief about the relative performance of A versus B . For ordinal data, this has the implication that pairwise comparisons are the primitive unit; a full ranking over n items is then simply a consistent encoding of all $\binom{n}{2}$ pairwise comparisons. For a single pair $\{A, B\}$, the only meaningful quantity is how often A beats B , or more generally, the win probability $P(A > B)$. Any measure that treats ranks as cardinal (e.g., Borda scores or expected rank) assigns meaning to rank differences, which depend on the number of items present and therefore violate IIA. Notably, win probabilities are a fair attribution scheme by construction, i.e., are additive by mutual exclusivity of winning and satisfy Shapley properties such as efficiency, symmetry, and marginality. Win probabilities are thus the canonical measure for ordinal data under IIA.

Crucially, rankings aggregate coherently across arbitrary instance distributions. Let \mathcal{J} denote a distribution over problem instances. For each instance $I \sim \mathcal{J}$, a ranking over algorithms \mathbf{A} is observed. Pooling these rankings estimates the marginal win probability:

$$\theta_A = \mathbb{E}_{I \sim \mathcal{J}}[P(A \text{ ranks first within } \mathbf{A} \mid I)]. \quad (1)$$

This is true marginalization: the quantity θ_A has a direct interpretation as the probability that algorithm A is best in \mathbf{A} on a random draw from \mathcal{J} . In contrast, averaging normalized objective values across instances yields a number with no clear probabilistic or decision-theoretic meaning.

The preceding argument applies at each timepoint. At time t , algorithm A is preferred to B if it wins more often:

$$A \succ^t B \iff \theta_A(t) > \theta_B(t), \quad (2)$$

where $\theta_A(t)$ denotes the marginal win probability of algorithm A at time t across the instance distribution \mathcal{J} . Different algorithms may be preferred with different available budgets. An algorithm that converges quickly may dominate early, while a more exploratory algorithm may dominate at longer runtimes. Both represent valid strategies, and which one is preferable depends on the user's time preference.

We therefore define anytime dominance as dominance across all timepoints:

$$A \succ^{\mathcal{J}} B \iff A \succ^t B \forall t \in \mathcal{T}. \quad (3)$$

An algorithm that is anytime-dominated is inferior regardless of how the user values time: no matter which timepoints are of interest, there exists another algorithm strictly better everywhere. Note that we write strict inequality throughout for simplicity, since equal win probabilities occur with probability zero for continuous density over θ (cf. Section 3.1), i.e., happen *almost never*.

The *anytime Pareto set* consists of all algorithms not anytime-dominated by any other:

$$\mathcal{P} = \{A : \nexists B \in \mathbf{A} \text{ s.t. } B \succ^{\mathcal{J}} A\}. \quad (4)$$

This set contains exactly the algorithms that are optimal under some preference functional over time. Collapsing to a single “best” algorithm requires specifying such a preference; the Pareto set is the minimal output that supports any such choice.

While we focus on single-objective black-box optimization in this paper, the framework applies wherever algorithms can be ranked. Reinforcement learning (RL) agents can be compared by expected episode return; multi-objective optimizers and multi-objective RL methods by hypervolume or expected utility under a weight distribution. These latter metrics induce total orders over otherwise incomparable outcomes, which reintroduce domain assumptions: hypervolume requires a reference point, expected utility requires a weight prior, trading the full scale-free property for applicability to partial-order settings. We leave native treatment of partial orders to future work.

3 Bayesian Plackett-Luce Models for Anytime Performance Analysis

The previous section has established that win probabilities are the canonical measure for ordinal comparison under IIA. We now require a model for inference. The Bradley-Terry model [Bradley and Terry 1952] directly parameterizes pairwise win probabilities: given ratings $\theta_A(t), \theta_B(t) > 0$, the probability that A beats B at time t is

$$P(A \succ^t B) = \frac{\theta_A(t)}{\theta_A(t) + \theta_B(t)}. \quad (5)$$

Bradley-Terry handles pairwise comparisons, but we observe full rankings: running n algorithms on an instance yields an ordering of all n for each t , not just a single pair. A full ranking encodes

$\binom{n}{2}$ pairwise outcomes that are mutually consistent. These cannot simply be treated as independent Bradley-Terry observations, since they derive from a single run. Obtaining truly independent pairwise comparisons under Bradley-Terry would require $2\binom{n}{2} = n(n-1)$ separate runs, each comparing only one pair. This makes Bradley-Terry statistically inefficient for our setting.

The Plackett-Luce (PL) model [Plackett 1975] extends Bradley-Terry to full rankings while preserving the pairwise win probability structure. Consider n algorithms with ratings $\theta(t) = (\theta_1(t), \dots, \theta_n(t))$, constrained to the probability simplex: $\theta_i(t) \geq 0$ and $\sum_i \theta_i(t) = 1 \forall t$. The probability of observing ranking $\pi = (\pi_1, \pi_2, \dots, \pi_n)$ at time t , where π_k denotes the algorithm in position k , follows a sequential choice process:

$$P(\pi | \theta(t)) = \prod_{k=1}^n \frac{\theta_{\pi_k}(t)}{\sum_{j=k}^n \theta_{\pi_j}(t)}. \quad (6)$$

First place is drawn with probability proportional to ratings; second place is drawn from the remaining alternatives proportionally; and so on. This process extends naturally to partial rankings where only the top $m < n$ positions are observed. We denote the set of all observed rankings as \mathcal{R} , with individual rankings $r \in \mathcal{R}$. Each ranking r is associated with a timepoint t_r and a weight w_r (equal to 1 by default). The full likelihood is:

$$P(\mathcal{R} | \theta) = \prod_{r \in \mathcal{R}} P(r | \theta(t_r))^{w_r}. \quad (7)$$

The key property is that PL preserves the Bradley-Terry pairwise structure: marginalizing over all other algorithms recovers $P(A \succ^t B) = \theta_A(t) / (\theta_A(t) + \theta_B(t))$. This is IIA, directly following from Luce's choice axiom [Luce 1959]: the pairwise win probability depends only on A and B , not on which other algorithms are present, and adding or removing algorithms does not change inference about any pair.

The PL model admits an equivalent characterization through latent utilities. Each algorithm i has a true quality $\mu_i(t)$, and on each comparison a noisy utility $U_i(t) = \mu_i(t) + \epsilon_i$ is realized, where ϵ_i are independent draws from a standard Gumbel distribution. Algorithms are ranked by their realized utilities. This Thurstonian interpretation yields the PL model with $\theta_i(t) = \exp(\mu_i(t)) / \sum_j \exp(\mu_j(t))$. The interpretation is intuitive: algorithms have fixed latent qualities, but observed performance is subject to independent random variation.

When multiple algorithms can be executed in parallel, the relevant question shifts from "which algorithm is best?" to "which combination is best?". The PL model provides a natural answer through its Thurstonian interpretation, since the maximum of independent Gumbel random variables is itself Gumbel-distributed, with location parameter equal to the log-sum-exp of the individual locations. In terms of ratings, this means the probability that the best algorithm in a portfolio S at time t beats the best algorithm in portfolio S' at time t is:

$$P(\max_{i \in S} U_i(t) > \max_{j \in S'} U_j(t)) = \frac{\sum_{i \in S} \theta_i(t)}{\sum_{i \in S} \theta_i(t) + \sum_{j \in S'} \theta_j(t)}. \quad (8)$$

The portfolio rating $\theta_S(t) = \sum_{i \in S} \theta_i(t)$ is simply the sum of individual ratings, interpreted as the probability that the portfolio contains the overall winner. This aggregation is coherent when quality is max-aggregated: running algorithms in parallel yields the maximum of their individual outcomes. It holds whenever the user takes the single best solution found, i.e., the solution with the lowest objective value or highest expected return. For hypervolume and related indicators in multi-objective optimization, the property does not hold in general, since the hypervolume of combined

Pareto fronts can exceed the maximum of the individual hypervolumes when fronts cover complementary regions of the objective space:

$$\text{HV}\left(\bigcup_{i \in S} P_i\right) \geq \max_i \text{HV}(P_i). \quad (9)$$

The sum formula then underestimates the true portfolio value. However, this can be addressed without additional experiments by computing the joint hypervolume from existing Pareto fronts and introducing the portfolio as a virtual algorithm in the ranking model. IIA ensures that existing inference remains valid when algorithms are added. Note that portfolio comparisons are generally only meaningful under fixed parallel budget. Comparing a size- k portfolio against a single algorithm conflates algorithmic quality with parallelization advantage; fair comparison requires all candidates to use the same number of parallel slots.

The PL likelihood assumes a strict total order, meaning that no two algorithms achieve identical performance. For continuous objective values, exact ties happen mathematically *almost never*. However, for example when multiple algorithms converge to the same optimum up to machine precision (common on easy problems with sufficient budget), or when objective values are discretized, tied positions arise. We handle these ties by expansion, following [Rojas-Delgado et al. 2022]: a k -way tie is replaced by all $k!$ possible orderings of the tied algorithms, each weighted with $w_r = 1/k!$. This preserves the expected contribution to the likelihood. When k is large, enumerating all $k!$ orderings is impractical. We then subsample a tractable amount uniformly from the set of permutations, which introduces additional variance but no bias. However, if the data contains many ties, the expanded rankings may still significantly slow down inference. An alternative approach introduces additional parameters encoding the probability of k -way ties [Turner et al. 2020]. While this handles ties natively within the likelihood, it loses algorithm-wise IIA: the probability that A beats B depends on whether C is involved in a tie with either. For our use case, this tradeoff is unfavorable.

3.1 Why Bayesian?

In practice, we observe a finite number of rankings \mathcal{R} on a set of instances $\mathbf{I} = \{I_1, I_2, \dots, I_p\}$ sampled from an instance distribution \mathcal{I} at timepoints $\mathbf{T} = (t_1, t_2, \dots, t_T)$, and wish to infer the latent ratings $\theta = (\theta(t_1), \theta(t_2), \dots, \theta(t_T))$. A point estimate $\hat{\theta}$, such as the maximum likelihood estimate, provides no measure of uncertainty. With limited data, two algorithms may have similar empirical win rates, but we cannot know from $\hat{\theta}$ alone whether this reflects true equivalence or insufficient evidence.

The Bayesian approach treats θ as a random variable and computes the posterior distribution given observed rankings \mathcal{R} :

$$P(\theta \mid \mathcal{R}) \propto P(\theta) \prod_{r \in \mathcal{R}} P(r \mid \theta)^{w_r}, \quad (10)$$

where $P(\theta)$ is a prior distribution encoding beliefs before observing data. The posterior directly answers the questions we care about: What is the probability that algorithm A is better than B at time t ? How confident are we in this probability? This uncertainty quantification is essential for sequential decision-making, for example about anytime dominance. The Bayesian posterior provides the natural tool: we act when $P(\theta_B(t) > \theta_A(t) \mid \mathcal{R})$ exceeds a decision threshold, i.e., when our belief is sufficiently concentrated. This is the probability we actually care about, namely how confident we are that B dominates A given what we have observed.

Frequentist approaches to the same problem yield p-values: the probability of observing data at least as extreme as what was observed, assuming a null hypothesis. This is not the probability that the null is true, and the distinction matters for decision-making. A p-value of 0.01 does not

Table 1. Temporal Plackett-Luce model variants for anytime performance analysis.

Model	Prior structure	Space	Temporal	Complexity in T
Independent Dirichlet	$\theta(t) \sim \text{Dir}(\alpha)$	Simplex	Independent	$O(T)$
Hierarchical Dirichlet	$\theta(t) \sim \text{Dir}(\kappa/n)$, shared κ	Simplex	Independent	$O(T)$
Gaussian Process (GP)	$\eta_q \sim \mathcal{GP}(0, k)$	Log	Smooth	$O(T^3)/O(T^2M)$
Hilbert Space GP	$\eta_q \approx \sum_j \beta_j \phi_j$	Log	Smooth	$O(Tm)$
Random Walk	$\eta_q(t_{i+1}) \sim \mathcal{N}(\eta_q(t_i), \sigma^2 \Delta t)$	Log	Markov	$O(T)$
B-spline	$\eta_q = \sum_j \beta_j B_j$	Log	Smooth	$O(TK)$

Notes: T = number of timepoints, M = inducing points, m = HSGP basis functions, K = spline knots.

mean there is a 1% chance the null is true; a posterior probability of 0.99 for dominance does mean, given the model and data, we believe dominance holds with 99% probability.

A common concern with multiple comparisons in frequentist inference is the accumulation of Type I errors: testing many pairs at significance level α leads to an expected number of false positives proportional to the number of tests. Corrections such as Bonferroni or Holm adjust significance thresholds to control family-wise error rates. In the Bayesian framework, this concern does not arise in the same form. Each posterior probability is a coherent belief conditional on model and data. Computing many posteriors does not degrade any individual one; there is no “alpha to spend”. If we wish to know the probability of at least one erroneous elimination, we can compute it directly from the joint posterior rather than applying a correction to thresholds. The guarantees are conditional on the model being well-specified, specifically that the PL model adequately describes the data-generating process. However, given that we observe only rankings and require IIA, the PL model is not one choice among many but the canonical model for this data structure.

3.2 Priors and Models

The prior $P(\theta)$ determines how information is shared across timepoints and encodes assumptions about the structure of algorithm performance over time. We present a hierarchy of models ranging from fully independent to smoothly correlated, an overview of which is given in Table 1.

Two parameterizations of θ are natural. The first works directly on the simplex: $\theta(t) \in \Delta^{n-1}$ with Dirichlet priors. The second works in log-space: define unconstrained utilities $\mu(t) \in \mathbb{R}^n$ with $\theta(t) = \text{softmax}(\mu(t))$, and place priors on μ . The log-space parameterization is more flexible for temporal modeling, since stochastic processes and related constructions usually apply directly to unconstrained real values. Since the PL likelihood depends only on differences $\mu_i(t) - \mu_j(t)$ in log-space, not absolute values, adding a constant to all utilities leaves the likelihood unchanged. For identifiability of unconstrained utilities, we impose a sum-to-zero constraint: $\sum_i \mu_i(t) = 0$ for all t . This is implemented via the Helmert matrix $Q \in \mathbb{R}^{n \times (n-1)}$, which maps $n - 1$ unconstrained latent functions $\eta_q(t)$ to n utility functions satisfying the constraint [Lancaster 1965]. We place identical priors on η_q ; the Helmert transformation ensures identifiability without affecting the likelihood. Note that the individual latent functions η_q do not map to specific algorithms; the Helmert transformation $\mu(t) = Q\eta(t)$ combines them into algorithm-specific utilities. More details on the Helmert matrix are given in Section A.

3.2.1 Independent Models. Our simplest prior treats timepoints as independent and exchangeable. Under the Dirichlet model, $\theta(t) \sim \text{Dirichlet}(\alpha, \dots, \alpha)$ independently for each t , where $\alpha > 0$ controls concentration. Small α favors concentration on a few algorithms; large α favors uniform

ratings. A hierarchical variant shares concentration across timepoints: $\kappa \sim \text{Exponential}(\lambda)$ and $\theta(t) \sim \text{Dirichlet}(\kappa/n, \dots, \kappa/n)$. This pools information about the overall level of differentiation among algorithms while maintaining conditional independence across time. These independent models are appropriate when timepoints are few or when no temporal structure is expected. A practical advantage of the independent Dirichlet model is that inference is embarrassingly parallel: each timepoint can be processed separately, also making it attractive for very large T .

3.2.2 Temporal Models. When performance evolves smoothly over time, temporal models improve statistical efficiency by sharing information across neighboring timepoints. We consider three constructions, all specified on the unconstrained latent functions $\eta_q(t)$.

Gaussian Process (GP). We model η via independent GPs:

$$\eta_q(\cdot) \sim \mathcal{GP}(0, k(\cdot, \cdot)), \quad (11)$$

where $k(t, t') = \sigma^2 K(t, t'; \ell)$ is a covariance kernel controlling smoothness, with amplitude σ and lengthscale ℓ . The lengthscale ℓ controls the rate of temporal variation: small ℓ allows rapid fluctuations, large ℓ enforces slow changes. Priors on σ and ℓ are weakly informative, using a log-normal and inverse gamma prior, respectively.

We use the Matérn class of kernels [Rasmussen and Williams 2005]:

$$C_\nu(t, t'; \ell) = \frac{2^{1-\nu}}{\Gamma(\nu)} \left(\sqrt{2\nu} \frac{|t - t'|}{\ell} \right)^\nu K_\nu \left(\sqrt{2\nu} \frac{|t - t'|}{\ell} \right), \quad (12)$$

where K_ν is the modified Bessel function of the second kind, and ν is a positive parameter that controls smoothness. Common choices are:

- Matérn-3/2 ($\nu = 3/2$): once differentiable, allowing moderately rough functions.
- Matérn-5/2 ($\nu = 5/2$): twice differentiable, smoother than Matérn-3/2.
- Squared exponential ($\nu \rightarrow \infty$): infinitely differentiable, very smooth.

The kernel choice encodes prior beliefs about temporal smoothness: Matérn-3/2 allows rougher trajectories with less regular curvature, while Matérn-5/2 enforces smoother transitions with continuous curvature. The squared exponential kernel assumes that performance evolves in a highly regular, infinitely smooth manner. We recommend Matérn-3/2 as the default choice, with Matérn-5/2 when smoother evolution is expected. The squared exponential kernel should be used with caution; its assumption of infinite differentiability is rarely justified in practice and should only be applied with compelling justification.

Inference of GPs scales cubically in the number of timepoints, which becomes prohibitive for large T . We use two approximation strategies to address this:

- (1) The sparse GP with inducing points [Quiñero-Candela and Rasmussen 2005] uses a set of $M < T$ inducing locations $\{\tilde{t}_1, \dots, \tilde{t}_M\}$ to approximate the full GP. The function values at the inducing points serve as a low-rank bottleneck, reducing complexity to $O(TM^2)$. We use the Deterministic Training Conditional (DTC) approximation and place the inducing points uniformly across data quantiles. This approach works well when a moderate number of inducing points capture the essential variability.
- (2) The Hilbert Space Gaussian Process (HSGP) [Riutort-Mayol et al. 2022] approximation exploits the spectral representation of stationary covariance functions. For a stationary kernel on a bounded domain $[0, L]$, the covariance function admits an eigendecomposition:

$$k(t, t') = \sum_{j=1}^{\infty} s_k(\sqrt{\lambda_j}) \phi_j(t) \phi_j(t'), \quad (13)$$

where ϕ_j and λ_j are eigenfunctions and eigenvalues of the Laplacian operator with Dirichlet boundary conditions, and s_k is the spectral density of the kernel k . The HSGP truncates this expansion after m terms:

$$\eta_q(t) \approx \sum_{j=1}^m \beta_{q,j} (s_k(\sqrt{\lambda_j}))^{\frac{1}{2}} \phi_j(t), \quad (14)$$

where $\beta_{q,j} \sim \mathcal{N}(0, 1)$ are independent coefficients. The boundary L is chosen as $L = c \cdot t_T$ where $c > 1$ is an extension factor that reduces boundary effects. The number of basis functions m and boundary extension c are chosen using the heuristics given by Riutort-Mayol et al. [2022], which select values based on the kernel type, domain size, and expected length-scale range to achieve a specified approximation accuracy. Larger m improves the approximation but increases computational cost. The approximation reduces inference complexity from $O(T^3)$ to $O(Tm + m)$, making it practical for hundreds or thousands of timepoints while preserving the GP's covariance structure.

Random Walk. An alternative for discrete timepoints is the Gaussian random walk:

$$\eta_q(t_{i+1}) \mid \eta_q(t_i) \sim \mathcal{N}(\eta_q(t_i), \sigma^2 \Delta t_i) \quad (15)$$

where $\Delta t_i = t_{i+1} - t_i$. This is a Markov model: the future depends on the past only through the present. The innovation variance σ^2 controls smoothness. Random walks are computationally efficient and appropriate when the temporal grid is fixed and dynamics are local.

B-spline. The third option represents each latent function as a linear combination of B-spline basis functions:

$$\eta_q(t) = \sum_{j=1}^K \beta_{q,j} B_j(t), \quad (16)$$

where B_j are B-spline basis functions of degree d (typically $d = 3$ for cubic splines) and $\beta_{q,j}$ are coefficients with Gaussian priors. By default, we choose $K = T/2$. The number and placement of the $K + d + 1$ knots control flexibility. B-splines are computationally efficient and allow localized control over smoothness, but require choosing the knot sequence. We place knots at quantiles of the observed timepoints, which adapts to the data density, similar to the inducing points.

3.2.3 Model Choice. The choice between independent and temporal models reflects assumptions about the data-generating process. Independent models assume no relationship between timepoints; temporal models assume smooth evolution. If temporal structure exists but is not modeled, posteriors remain valid but wider than necessary. If smooth evolution is assumed but violated, temporal models may be overconfident. When in doubt, independent models trade efficiency for robustness to misspecification. However, even under independent priors, posteriors exhibit smoothness across time. This arises from the data: rankings at adjacent timepoints derive from the same underlying trajectories, and best-so-far values change only when an algorithm finds an improvement. Temporal models encode this smoothness explicitly in the prior, while independent models let it emerge from the data. Beyond assumptions, the models differ in what queries they support. Independent models yield marginal posteriors at each timepoint; temporal models yield a joint posterior across time. Only the latter supports queries about simultaneous events, such as the probability that one algorithm is better at all timepoints. When such joint statements are required, temporal models are necessary regardless of efficiency considerations.

3.3 Computational Inference

Given observed rankings \mathcal{R} and a prior $P(\theta)$, we require samples of the posterior $P(\theta \mid \mathcal{R})$. We consider several inference strategies, trading accuracy against computational cost:

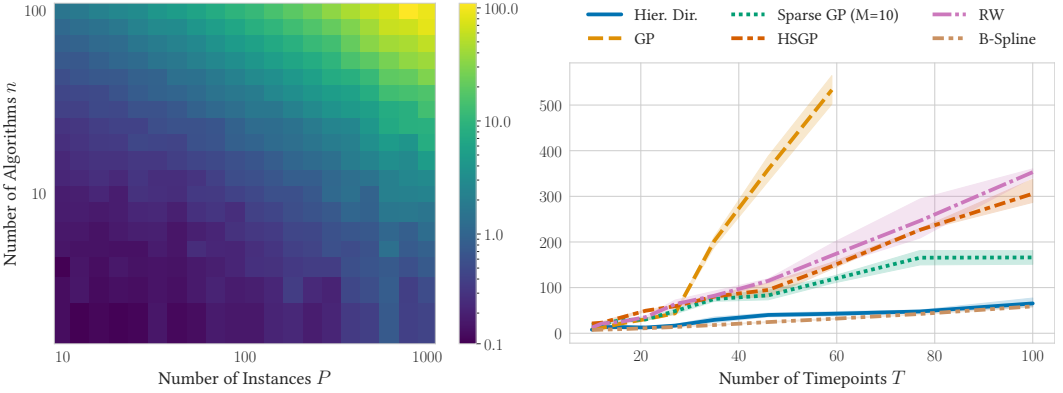
- Markov Chain Monte Carlo (MCMC) methods provide asymptotically exact posterior samples and are the gold standard for accuracy. Hamiltonian Monte Carlo (HMC) [Neal 2011] with the No-U-Turn Sampler (NUTS) [Homan and Gelman 2014] is state of the art for sampling complex posteriors of continuous parameters.
- Automatic Differentiation Variational Inference (ADVI) [Kucukelbir et al. 2017] approximates the posterior with a simpler family (typically Gaussian) by minimizing the Kullback-Leibler divergence. We differentiate between meanfield and fullrank ADVI, using a fully factorized Gaussian and Gaussian with a full-rank covariance matrix for the approximation, respectively.
- The Laplace approximation constructs a Gaussian centered at the maximum a posteriori (MAP) estimate, with covariance given by the inverse Hessian of the negative log-posterior [Tierney and Kadane 1986]. This is fast (requiring only optimization) and accurate when the posterior is approximately Gaussian.
- Pathfinder [Zhang et al. 2022] is a recent method that traces multiple optimization paths to the MAP, constructs sequences of Gaussian approximations along the way, and merges them using importance resampling. It combines the speed of optimization-based methods with improved robustness over Laplace.

We observe rankings at a discrete grid of timepoints $\mathbf{T} = (t_1, \dots, t_T)$. The endpoints t_1 and t_T define the interval of interest; the intermediate points control the resolution at which performance is tracked. We find that for most applications, a uniform or log-spaced grid of $T \in [10 \dots 100]$ timepoints suffices. Finer grids increase computational cost, while coarser grids risk missing rapid transitions. In principle, one could adaptively place timepoints where ranking order changes, preserving full information with minimal redundancy. We have not found this necessary in practice.

We provide implementations¹ of all models in PyMC [Abril-Pla et al. 2023], with both independent models and the full GP also being available in Stan [Stan Development Team 2026].

Overall computational cost depends on three factors: number of unique timepoints T , number of algorithms n , and number of sampled instances P , giving $|\mathcal{R}| = P \cdot T$. For MCMC, cost additionally depends on posterior geometry: correlated, curved, or multimodal posteriors require more conservative exploration. In HMC/NUTS this typically means smaller step sizes and longer trajectories, so each posterior sample uses more leapfrog steps (more gradient evaluations) and mixes more slowly. PyMC supports multiple execution backends (JAX, Numba) and sampler backends (NumPyro, BlackJAX, nutpie). In our experience, the PyMC implementation with JAX backend and NumPyro sampler provides the fastest execution time of all MCMC samplers (including Stan’s sampler). We emphasize that this may, however, change on different hardware or package versions. We also find that PL posteriors of the independent Dirichlet model are typically well-behaved, near-Gaussian with moderate correlation, making Pathfinder and Laplace reliable approximations. Inference for this model is embarrassingly parallel across timepoints. For typical benchmarking scenarios ($n \leq 30, P \leq 100$), inference remains under 10 seconds per timepoint using Stan’s Pathfinder (see Figure 1a), being about one order of magnitude faster than MCMC at indistinguishable quality. PyMC’s Pathfinder generally provides speedups over MCMC for most temporal models with only slightly to moderately degraded posteriors. However, we observe that Pathfinder fails to produce reliable approximations for the HSGP and random walk models, likely

¹The code is provided to reviewers and will be released under an open-source license upon publication.



(a) Pathfinder approximation of the independent Dirichlet model for a single timepoint, on a single CPU core. Note the log-scale on all axes.

(b) Temporal PL models for $n = 5$ and $P = 30$, using MCMC with 4 chains, 4 cores, 1000 warmup samples and 2000 posterior samples per chain.

Fig. 1. Mean execution time in seconds (5 repetitions) for selected models and approximation methods.

due to the strong posterior correlations induced by their parameterizations. For these models, we recommend MCMC. ADVI underperforms in our (arguably limited) experiments, and contrary to conventional expectations, tends to overestimate uncertainty compared to MCMC even when clearly converged (verified by monitoring the evidence lower bound (ELBO)). This happens for both the meanfield and fullrank variants.

Figure 1b shows how execution time increases with the number of considered timepoints T for a synthetic benchmarking setup with $n = 5$ algorithms and $P = 30$ instances, using MCMC for all models. The full GP exhibits the expected cubic scaling, exceeding 500 seconds by $T = 60$ and becoming impractical for finer grids. The sparse GP approximation with $M = 10$ inducing points offers meaningful improvement, reaching approximately 180 seconds at $T = 100$. HSGP and the random walk show similar performance at around 300 seconds for $T = 100$. The B-spline model is fastest among the temporal-aware options, staying below 100 seconds even at $T = 100$, together with the hierarchical Dirichlet. These timings represent a single slice of the parameter space ($n = 5$, $P = 30$); relative performance may differ for other configurations and data. The results also illustrate that asymptotic complexity (e.g., $O(T)$) can be misleading in practice, and that constant factors and implementation details matter substantially. We therefore recommend treating these benchmarks as indicative rather than definitive, and suggest users should profile on their specific problem size before committing to a model. Note the standard practice for MCMC diagnostics to ensure unbiased posteriors: $\hat{R} < 1.01$, ESS > 400 per parameter, no divergent transitions. For approximate methods, we recommend spot-checking against MCMC on representative subproblems. For general guidance on Bayesian workflows we refer to [Gelman et al. 1995; Vehtari et al. 2021], as well as the documentation of Stan² and PyMC³.

4 POLARBEAR: Pareto-Optimal Anytime Algorithms via Bayesian Racing

At deployment, the practitioner’s preference over budgets can be encoded as a functional $u : \mathbb{R}^T \rightarrow \mathbb{R}$ that aggregates performance across time. Given algorithms $\mathbf{A} = \{A_1, \dots, A_n\}$ with win

²<https://mc-stan.org/docs/>

³<https://www.pymc.io>

probabilities $\theta(t)$, the value of algorithm A under u is:

$$V_A^u = u(\theta_A(t_1), \dots, \theta_A(t_T)). \quad (17)$$

We restrict attention to strictly monotonically increasing preferences: u is strictly monotonically increasing if $\theta(t) > \theta'(t)$ for all t implies $u(\theta) > u(\theta')$. This captures the intuition that higher win probability is always better: no reasonable preference is indifferent to, or even penalizes, an algorithm for being more likely to win everywhere. When u is known, the selection problem reduces to estimating θ with sufficient precision to identify $A_u^* = \arg \max_A V_A^u$. When u is unknown at benchmarking time, we ask: what is the minimal output that supports selection under *any* strictly monotonically increasing u ?

Let \mathcal{U} denote the class of strictly monotonically increasing preference functionals. This class includes weighted integrals $u(\theta) = \int w(t)\theta(t) dt$, $w(t) \geq 0 \forall t$, budget distributions $u(\theta) = \mathbb{E}_{t \sim \mathcal{B}}[\theta(t)]$ for any distribution \mathcal{B} , final-time preference $u(\theta) = \theta(t_T)$, and arbitrary strictly monotonic compositions thereof.

PROPOSITION 4.1. *Algorithm A is optimal under some $u \in \mathcal{U}$ if and only if $A \in \mathcal{P}$.*

PROOF. (\Rightarrow) Suppose $A \notin \mathcal{P}$, i.e., A is dominated by some B . Then $\theta_B(t) > \theta_A(t)$ for all t . For any strictly monotonically increasing u , this implies $u(\theta_B) > u(\theta_A)$, so A is not optimal.

(\Leftarrow) Suppose $A \in \mathcal{P}$, i.e., A is non-dominated. Define the preference functional:

$$u^*(\theta) = \min_t (\theta(t) - \theta_A(t)). \quad (18)$$

This is strictly monotonically increasing: if $\theta(t) > \theta'(t)$ for all t , then $\theta(t) - \theta_A(t) > \theta'(t) - \theta_A(t)$ for all t . Let $t^* = \arg \min_t (\theta(t) - \theta_A(t))$. Then:

$$u^*(\theta) = \theta(t^*) - \theta_A(t^*) > \theta'(t^*) - \theta_A(t^*) \geq \min_t (\theta'(t) - \theta_A(t)) = u^*(\theta'). \quad (19)$$

- For algorithm A : $u^*(\theta_A) = \min_t (\theta_A(t) - \theta_A(t)) = 0$.
- For any $B \neq A$: since A is non-dominated, B does not dominate A , so there exists t^* with $\theta_B(t^*) \leq \theta_A(t^*)$. Thus, $u^*(\theta_B) = \min_t (\theta_B(t) - \theta_A(t)) \leq \theta_B(t^*) - \theta_A(t^*) \leq 0$.

Therefore, $u^*(\theta_A) = 0 \geq u^*(\theta_B)$ for all $B \neq A$, so A is optimal under u^* . \square

The Pareto set \mathcal{P} is therefore the minimal sufficient output, since it contains exactly the algorithms that could be optimal for some user, and excluding any non-dominated algorithm would preclude optimality for some preference. Conversely, dominated algorithms are suboptimal regardless of how the user values time.

However, \mathcal{P} depends on the true win probabilities θ , which are unknown. We observe only rankings from a finite number of experimental runs, which induces uncertainty about Pareto membership. For some algorithms, we may be confident they are dominated; for others, confident they are non-dominated; for yet others, uncertain. A naive approach runs all algorithms for a fixed number of instances, and reports the posterior, allocating samples uniformly regardless of which comparisons are already resolved. We seek instead to identify \mathcal{P} using as few experiments as possible, and minimizing experimental cost requires adaptive decision-making. This means that after each batch of experiments, we update our beliefs and decide what to run next, which is exactly the setting of sequential Bayesian experimental design. At each round, we observe rankings, update the posterior over θ , and choose which algorithms to sample further. The IIA property of the Plackett-Luce model gives this procedure a particular structure, since inference about the pair $\{A, B\}$ is unaffected by the presence or absence of other algorithms:

- (1) An algorithm can be eliminated once it is confidently dominated, and future samples need not include it.

- (2) Eliminating an algorithm does not invalidate inference about remaining algorithms.
- (3) New algorithms can be added at any time without affecting existing posteriors; they enter with the prior and are updated by new observations.

Sequential Bayesian inference under IIA thus naturally yields a racing procedure where algorithms compete, losers are eliminated when confidently dominated, and sampling continues among the survivors. We call this procedure POLARBEAR⁴.

It remains to specify when to terminate the race, i.e., at which point we have gathered enough information to support confident selection for arbitrary preferences. We formalize this through regret, or the cost incurred by selecting a suboptimal algorithm. Given posterior $P(\theta \mid \mathcal{R})$, selecting algorithm A under preference u incurs expected regret:

$$\text{Regret}(A, u) = \mathbb{E} \left[\max_{A'} V_{A'}^u - V_A^u \mid \mathcal{R} \right], \quad (20)$$

where $P(V_A^u \mid \mathcal{R})$ is constructed by propagating posterior samples of θ through u . When u is unknown, we consider worst-case regret over \mathcal{U} :

$$\sup_{u \in \mathcal{U}} \min_{A \in \hat{\mathcal{P}}} \text{Regret}(A, u), \quad (21)$$

where $\hat{\mathcal{P}}$ is our current estimate of the Pareto set. This regret decomposes into two components, namely *reducible* and *irreducible* regret. The former encodes uncertainty about pairwise orderings $\theta_A(t) \geq \theta_B(t)$, which decreases with additional samples as posteriors concentrate. The latter is the preference ambiguity among true Pareto members. For any two distinct non-dominated algorithms A and B , there exist $u, u' \in \mathcal{U}$ with $V_A^u > V_B^u$ and $V_B^{u'} > V_A^{u'}$, and no amount of data resolves which is “better” without knowing u . Consequently, we aim to minimize the reducible regret, which we achieve by determining all pairwise orderings with high certainty, so that remaining uncertainty reflects only the user’s unspecified preference. Specifically, POLARBEAR terminates when, for every pair of candidate algorithms and every timepoint, the posterior confidently determines their relation. This is deliberately conservative, expressing the intuitive sentiment that, at this point, the cost of additional experiments is greater than the potential gain in information, no matter the preference.

4.1 Confidence-Based Relations

The racing procedure requires decisions about the relation between two algorithms under uncertainty. We define two such relations: dominance (one algorithm is confidently better) and equivalence (neither is meaningfully better). We formalize these through posterior probabilities over pairwise win rates, calculated by counting the proportion of posterior samples satisfying the condition.

Dominance. Algorithm A α -dominates B at time t when the posterior concentrates on A having higher win probability:

$$A \stackrel{t}{\succ}_{\alpha} B \iff P \left(\frac{\theta_A(t)}{\theta_A(t) + \theta_B(t)} > 0.5 \mid \mathcal{R} \right) = P(\theta_A(t) > \theta_B(t) \mid \mathcal{R}) \geq \alpha, \quad (22)$$

where $\alpha \in (0.5, 1]$ is a decision threshold, typically 0.95 or 0.99. The win probability threshold is at 0.5, i.e., any credible advantage, however small, constitutes dominance. By symmetry,

$$P(\theta_A(t) > \theta_B(t) \mid \mathcal{R}) + P(\theta_B(t) > \theta_A(t) \mid \mathcal{R}) = 1. \quad (23)$$

⁴Pareto-optimal anytime algorithms via Bayesian racing

Anytime α -dominance is defined jointly for each $t \in \mathbf{T}$:

$$A \underset{\alpha}{\succ} B \iff P(\theta_A(t) > \theta_B(t) \forall t \in \mathbf{T} \mid \mathcal{R}) \geq \alpha. \quad (24)$$

Note that anytime α -dominance is strictly more conservative:

$$B \underset{\alpha}{\succ} A \implies B \underset{\alpha}{\succ}^t A, \quad (25)$$

but not conversely. Furthermore, since anytime dominance is a partial order, the above symmetry does not hold here.

Equivalence. Algorithms A and B are (ϵ, α) -equivalent at time t when the posterior concentrates on their pairwise win probability being near 0.5:

$$A \underset{\alpha}{\approx} B \iff P\left(\frac{\theta_A(t)}{\theta_A(t) + \theta_B(t)} \in [0.5 - \epsilon, 0.5 + \epsilon] \mid \mathcal{R}\right) \geq \alpha, \quad (26)$$

where $\epsilon \in [0, 0.5)$ defines the region of practical equivalence (ROPE) around 0.5, typically 0.05. This is analogous to the use of ROPE in Bayesian hypothesis testing [Kruschke 2018] but adapted to pairwise win probabilities. The parameter ϵ encodes the user's indifference: when we believe the pairwise win probability is within ϵ of even odds, the distinction is not decision-relevant (e.g., 0.45 to 0.55 for $\epsilon = 0.05$). Larger ϵ means a decision is easier to reach and declares more algorithms equivalent; smaller ϵ requires more evidence but distinguishes finer differences. Note that the earlier definition of α -dominance is not mutually exclusive with α -equivalence since the posterior can concentrate in $(0.5, 0.5 + \epsilon]$; for decision-making however, α -dominance \geq takes precedence.

4.2 Design Choices

POLARBEAR admits two orthogonal design choices: when to eliminate an algorithm and when to stop sampling an algorithm. These interact with model choice to yield different tradeoffs between statistical efficiency, computational cost, and the strength of output.

Elimination. The mode of elimination determines when an algorithm is considered dominated and subsequently removed from the candidate Pareto set:

- *Pointwise:* Algorithm A is eliminated if B α -dominates A at each timepoint t individually:

$$\exists B \in \mathbf{A} : \forall t \in \mathbf{T} : B \underset{\alpha}{\succ}^t A. \quad (27)$$

- *Joint:* Algorithm A is eliminated if B is better at all timepoints simultaneously:

$$\exists B \in \mathbf{A} : B \underset{\alpha}{\succ}^{\mathbf{T}} A. \quad (28)$$

Under pointwise elimination, each timepoint is tested separately. This is natural for independent models, where posteriors factorize across time (cf. Section 3.2.1). However, pointwise elimination can lead to premature elimination when posteriors are negatively correlated across timepoints. This occurs when uncertainty is about trajectory *shape* rather than *level*. If the posterior entertains both “ B better early, worse late” and “ B worse early, better late” scenarios, then the events “ B wins at t_1 ” and “ B wins at t_2 ” are negatively correlated. Marginally, B may appear to dominate at each timepoint with high probability, while the joint event “ B dominates everywhere” has substantially lower probability. Joint elimination avoids this pathology, requiring a joint posterior over all timepoints, which is available from temporal models (cf. Section 3.2.2).

Resolution. The resolution mode determines when to stop sampling an algorithm because its relationship with all other algorithms is sufficiently established. This is defined over pairwise resolution $\mathbf{C} : \mathbf{T} \times \binom{\mathbf{A}}{2} \mapsto \{\top, \text{F}\}$ at each t , where an algorithm A_i is resolved if all pairs involving A are resolved for all t :

$$A_i \text{ resolved} \iff \forall t \in \mathbf{T}, \forall A_j \in \mathbf{A} : \mathbf{C}(t, \{A_i, A_j\}) = \top. \quad (29)$$

All pairs involving an eliminated algorithm A are naturally marked as resolved. This follows from the semantics: A is dominated, so its relationship with every other algorithm is determined (inferior everywhere). Remaining algorithms need not be compared against A , and A 's elimination may cause other algorithms to become fully resolved if A was their only unresolved partner. We differentiate between two modes for the remaining pairwise resolution:

- *Strict:* A pair $\{A, B\}$ is resolved at t when we can be confident about some relation at t :

$$\mathbf{C}(t, \{A, B\}) = \top \iff (A \overset{t}{\succ}_{\alpha} B) \vee (B \overset{t}{\succ}_{\alpha} A) \vee (A \overset{t}{\approx}_{\alpha} B). \quad (30)$$

- *Crossing:* A pair $\{A, B\}$ is resolved early at all timepoints when evidence of crossing trajectories is detected, i.e., a pair is resolved if we are certain that A dominates (or ties) at some t and B dominates (or ties) at some t' , with at least one strict dominance:

$$\begin{aligned} \mathbf{C}(t, \{A, B\}) = \top \forall t \in \mathbf{T} \iff \\ \exists t, t' \in \mathbf{T} : (A \overset{t}{\succ}_{\alpha} B \vee A \overset{t}{\approx}_{\alpha} B) \wedge (B \overset{t'}{\succ}_{\alpha} A \vee A \overset{t'}{\approx}_{\alpha} B) \wedge (A \overset{t}{\succ}_{\alpha} B \vee B \overset{t'}{\succ}_{\alpha} A). \end{aligned} \quad (31)$$

The strict resolution mode requires confident determination of every pairwise relationship at every timepoint. This is necessary when the user may apply arbitrary preference functionals, since any timepoint could be decision-relevant. However, for the narrower goal of identifying Pareto set membership, strict resolution can be wasteful. Consider two algorithms with crossing trajectories: A is better early, B is better late. Once we are confident of this crossing, i.e., confident that A wins at some t_1 and B wins at some t_2 , we know neither can dominate the other. Both must remain in the Pareto set regardless of what happens at other timepoints. Continuing to sample this pair until all timepoints are resolved yields tighter posteriors but cannot change the Pareto membership conclusion. The crossing resolution is an extension of the strict resolution that exploits this structure. A pair is resolved early when evidence of crossing is detected: one algorithm confidently dominates (or ties) at some timepoint, the other confidently dominates (or ties) at another, with at least one strict dominance. This reduces sample cost when algorithms have genuinely different anytime profiles. The tradeoff is that crossing resolution guarantees only Pareto set membership, not tight posteriors everywhere. If a user's preference concentrates on specific timepoints, additional targeted sampling may be needed for final selection.

4.3 The Racing Procedure

Algorithm 1 summarizes the POLARBEAR procedure⁵. The algorithm maintains a candidate Pareto set $\hat{\mathcal{P}}$, initialized to all anytime algorithms under consideration, and iteratively samples, updates beliefs, eliminates dominated algorithms, and resolves pairwise relationships until all pairs in $\hat{\mathcal{P}}$ are resolved at all timepoints. We refer to a single such iteration as a *round*.

⁵The implementation of POLARBEAR is provided to reviewers and will be released upon publication as part of a broader open-source toolbox.

Algorithm 1: POLARBEAR

Input: Algorithms \mathbf{A} , timepoints \mathbf{T} , decision α , equivalence threshold ϵ , batch size b
Output: Pareto set $\hat{\mathcal{P}}$, posterior $P(\theta | \mathcal{R})$

- 1 $\hat{\mathcal{P}} \leftarrow \mathbf{A}$;
- 2 $\mathcal{R} \leftarrow \emptyset$;
- 3 $\mathbf{C}(t, \{A_i, A_j\}) \leftarrow \text{F}$ for all $t \in \mathbf{T}, \{A_i, A_j\} \in \binom{\mathbf{A}}{2}$;
- 4 **while** $\exists \{A, B\} \in \binom{\hat{\mathcal{P}}}{2}, t \in \mathbf{T} : \mathbf{C}(t, \{A, B\}) = \text{F}$ **do**
 - // Sample unresolved algorithms
 - 5 $\hat{\mathbf{A}} \leftarrow \{A \in \hat{\mathcal{P}} : \exists B \in \hat{\mathcal{P}}, t \in \mathbf{T} : \mathbf{C}(t, \{A, B\}) = \text{F}\}$;
 - 6 Sample b instances from \mathcal{J} , run algorithms in $\hat{\mathbf{A}}$;
 - 7 $\mathcal{R} \leftarrow \mathcal{R} \cup \{\text{new rankings}\}$;
 - // Update posterior
 - 8 Compute $P(\theta | \mathcal{R})$;
 - // Check elimination
 - 9 **foreach** $A \in \hat{\mathcal{P}}$ **do**
 - 10 **if** $\exists B \in \hat{\mathcal{P}} : B$ dominates A (pointwise or joint) **then**
 - 11 $\hat{\mathcal{P}} \leftarrow \hat{\mathcal{P}} \setminus \{A\}$;
 - 12 $\mathbf{C}(t, \{A, \cdot\}) \leftarrow \text{T}$ for all t ;
 - // Update resolution status
 - 13 **foreach** $\{A, B\} \in \binom{\hat{\mathcal{P}}}{2}$ **do**
 - 14 **foreach** $t \in \mathbf{T}$ **do**
 - 15 **if** $(A \stackrel{t}{>}_{\alpha} B) \vee (B \stackrel{t}{>}_{\alpha} A) \vee (A \stackrel{t}{\approx}_{\alpha} B)$ **then**
 - 16 $\mathbf{C}(t, \{A, B\}) \leftarrow \text{T}$;
 - // Crossing resolution (optional)
 - 17 **if** crossing detected for $\{A, B\}$ **then**
 - 18 $\mathbf{C}(t, \{A, B\}) \leftarrow \text{T}$ for all $t \in \mathbf{T}$;
- 19 **return** $\hat{\mathcal{P}}, P(\theta | \mathcal{R})$

Sampling Strategy. Pointwise elimination, while a weaker criterion than joint elimination, has the practical advantage that not all algorithms require evaluation at all timepoints. For each algorithm $A \in \hat{\mathcal{P}}$, we can define its maximum unresolved timepoint:

$$\tau_A = \max \left\{ t \in \mathbf{T} : \exists B \in \hat{\mathcal{P}}, \mathbf{C}(t, \{A, B\}) = \text{F} \right\}. \quad (32)$$

Once all pairs involving A are resolved at late timepoints, we can stop A earlier in subsequent rounds, reducing computational cost without losing information. Algorithms that are fully resolved are naturally not sampled at all.

Batch Size. Each round samples b new instances, running each unresolved algorithm A on each instance up to time τ_A . The choice of b trades off sample efficiency against computational overhead. At one extreme, $b = 1$ updates beliefs after every ranking trajectory. This minimizes algorithm

runs since sampling stops immediately when a pair resolves, with no wasted evaluations. However, this requires recomputing the posterior after each instance, and while inference is typically fast compared to algorithm execution, the overhead accumulates over many rounds. At the other extreme, large b amortizes inference cost over many instances and exploits parallel hardware. Modern compute environments increasingly favor batch execution; running $b \cdot |\hat{\mathcal{P}}|$ algorithm instances in parallel may take little more wall-clock time than running one. The cost is potential waste, as some runs may occur after a pair has effectively resolved, contributing no new information.

Adaptive batching offers a practical compromise. Some pairs resolve quickly with few samples; others, particularly nearly equivalent algorithms or those with subtle crossing behavior, may require substantially more evidence. While optimal batch sizing could be formulated as a decision-theoretic problem, we find a simple heuristic effective in practice: we double b when no pairs resolve in a round (indicating slow progress) and halve it when many (e.g., $> 20\%$) resolve (indicating diminishing returns from large batches), clipped to $[b_{\min}, b_{\max}]$. This allows the procedure to increase parallelism precisely when it is needed, reaching large batch sizes for difficult pairs while maintaining efficiency during early rounds when easy eliminations dominate. More sophisticated strategies could adapt b based on how close resolution of each pair is to its decision threshold α , or estimate the expected number of samples until resolution by simulating fantasy observations drawn from the current posterior. We leave such refinements to future work.

Early Termination. Note that the procedure can be preemptively terminated at any round. The current candidate set $\hat{\mathcal{P}}$ and posterior $P(\theta \mid \mathcal{R})$ are always valid, i.e., $\hat{\mathcal{P}}$ contains all algorithms not yet confidently dominated, and the posterior reflects all observed evidence. Early termination yields wider credible intervals and potentially unresolved pairs, but no bias. This is a general consequence of the Bayesian treatment: users with constrained experimental budgets can stop when posteriors are sufficiently concentrated for their purposes, even before the built-in termination criterion is met. The built-in criterion is deliberately conservative, ensuring that the reducible component of worst-case regret is driven toward zero.

Dynamically Adding Algorithms At Runtime. The IIA property of PL permits adding algorithms to the race at any time. A new algorithm A_{new} enters with the prior, joins $\hat{\mathcal{P}}$, and is marked unresolved against all existing candidates. Posterior beliefs about existing algorithms are unaffected; only new observations involving A_{new} update its rating. Specifically, A_{new} is first executed on a batch of cached instances previously sampled from \mathcal{J} , and then injected into the existing rankings, using the cached best-so-far trajectories of the existing algorithms. This can be repeated until it is either eliminated or catches up with the other Pareto candidates, at which point the race continues as before. This enables iterative workflows where initial racing identifies a preliminary Pareto set, and new candidates (e.g., generated by an automated algorithm design strategy) are introduced without restarting the analysis.

4.4 Algorithm Selection under Time Preferences and Risk Profiles

The output of POLARBEAR is a candidate Pareto set $\hat{\mathcal{P}}$ together with a concentrated posterior $P(\theta \mid \mathcal{R})$. This posterior supports selection under arbitrary time preferences and risk profiles, allowing fast and principled decision-making at deployment time.

Given a preference $u \in \mathcal{U}$, the posterior induces a distribution over values $P(V_A^u \mid \mathcal{R})$, computed by propagating posterior samples of θ through u . Different risk profiles correspond to different decision criteria over this distribution:

- *Probability of being best (P2BB)*: Select the algorithm most likely to be optimal:

$$A^* = \arg \max_{A \in \hat{\mathcal{P}}} P(V_A^u \geq V_B^u \forall B \in \hat{\mathcal{P}} \mid \mathcal{R}). \quad (33)$$

- *Expected value (risk-neutral)*: Select the algorithm with highest posterior mean:

$$A^* = \arg \max_{A \in \hat{\mathcal{P}}} \mathbb{E}[V_A^u \mid \mathcal{R}]. \quad (34)$$

- *Lower quantile (risk-averse)*: Select the algorithm with best worst-case performance at quantile level γ :

$$A^* = \arg \max_{A \in \hat{\mathcal{P}}} Q_\gamma[V_A^u \mid \mathcal{R}], \quad (35)$$

where Q_γ denotes the γ -quantile (e.g., $\gamma = 0.05$ for the 5th percentile).

All criteria are computed from posterior samples without additional experiments or inference. The choice of risk profile reflects the user's attitude toward uncertainty, i.e., risk-neutral users maximize expected performance, while risk-averse users protect against unfavorable outcomes.

When multiple algorithms can be deployed in parallel, the goal shifts from selecting a single algorithm to selecting a portfolio. As established in Section 3, the portfolio rating under the PL model is the sum of individual ratings when quality is max-aggregated:

$$\theta_S(t) = \sum_{A \in S} \theta_A(t), \quad (36)$$

representing the probability that the portfolio S contains the winner at time t , where multiplicity counts (running the same algorithm twice contributes twice its rating). The optimal portfolio of size k under preference u and decision criterion D is then:

$$S^* = \arg \max_{S \in \mathcal{M}_k(\hat{\mathcal{P}})} D[V_S^u \mid \mathcal{R}], \quad (37)$$

where $\mathcal{M}_k(\hat{\mathcal{P}})$ denotes all size- k multisets over $\hat{\mathcal{P}}$ and $V_S^u = u(\theta_S(t_1), \dots, \theta_S(t_T))$. For linear preferences (e.g., weighted integrals, budget distributions), the optimal size- k portfolio under expected value and probability of being best is the individually optimal algorithm repeated k times. After resolution, posteriors are sufficiently concentrated that quantile-based selection typically agrees. Other criteria and nonlinear preferences require evaluating portfolios jointly. For small k and $|\hat{\mathcal{P}}|$, exhaustive enumeration over all $\binom{|\hat{\mathcal{P}}|+k-1}{k}$ multisets is tractable. For larger cases, standard combinatorial optimization methods apply, such as greedy construction, simulated annealing, or iterated local searches. Since portfolio evaluation requires only summing over existing posterior samples and no additional inference, these methods can explore many candidates efficiently.

The selection criteria presented here condition on time preferences and risk profiles. This is orthogonal to traditional instance-based algorithm selection [Kerschke et al. 2019], which selects algorithms based on instance features. The two approaches are complementary: instance-based selection asks “given this problem, which algorithm?”, while anytime selection asks “given my budget preferences, which algorithm?”. Combining both axes, i.e., selecting based on instance features and time preferences jointly, is a natural extension that we leave to future work.

5 Case Studies

We evaluate POLARBEAR through three case studies. The first uses a synthetic ground truth to verify that the procedure correctly identifies Pareto sets and eliminates dominated algorithms. The second applies POLARBEAR to a classical benchmarking setup where traditional methods for anytime performance evaluation (EAF, ECDF, AOCC) are applicable, enabling direct comparison of

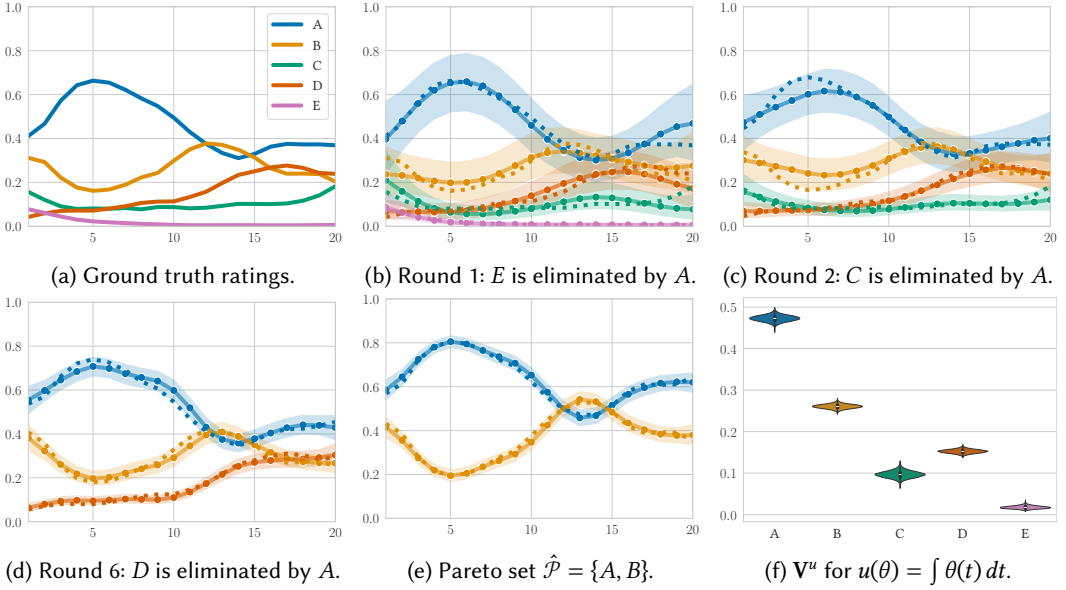


Fig. 2. A synthetic example with 5 algorithms. Figures (b) to (e) show the mean and 95% credible interval of the rating posterior (y-axis) over time (x-axis), with ground truth ratings from (a) as dotted lines. Figure (f) shows the resulting posterior over preference values for a uniform budget preference. Note that ratings at a specific t always sum to 1.

assumptions and conclusions. The third demonstrates a comparison under an arbitrary instance distribution where global optima are unknown, using wall-clock time rather than function evaluations as the budget axis. All experiments use a decision threshold of $\alpha = 0.99$ and equivalence threshold of $\epsilon = 0.05$. We use an initial batch size of $b = 8$, and the batch size adaptation heuristic with $b_{\min} = 8$ and $b_{\max} = 64$ for the first, and $b_{\max} = 128$ for the second and third case study.

5.1 Synthetic Ground Truth

We sample ground truth ratings θ^* from a Matérn prior with $\nu = 3/2$ and $\sigma \sim \text{Lognormal}(0, 0.5)$ and $\ell \sim \text{Inv-Gamma}(5, 3)$, with uniformly spaced timepoints. Rankings are generated by the Thurstonian interpretation: adding independent Gumbel noise to \log -ratings $\mu^* = \log \theta^*$ and ranking the result, which recovers the exact PL data-generating process, i.e., rankings with win probabilities θ^* . Inference uses the same model class, i.e., the GP model, but with a slightly different hyperprior of $\ell \sim \text{Inv-Gamma}(5, 2)$. We deliberately overestimate the rate of temporal variation here to show robustness against this kind of misspecification. Despite this mismatch, we expect correct Pareto set recovery as long as the model remains flexible enough to capture the true trajectory structure. We also vary the inference approach across examples, using the exact GP, HSGP and sparse GP with inducing points with different temporal resolution, showing that approximations can suffice. Elimination is done using joint dominance, with crossing algorithm pairs getting resolved early.

Example 1: Crossing Trajectories. The first example consists of 5 algorithms A to E , with $\mathcal{P} = \{A, B\}$ and $\{C, D, E\}$ being dominated by A . The ground truth rating trajectories are given in Figure 2a. We use the exact GP model with $T = 20$. The clearly inferior E and C are eliminated after round 1 and 2, or 8 and 16 instances, respectively. Algorithms A and D have close ratings for

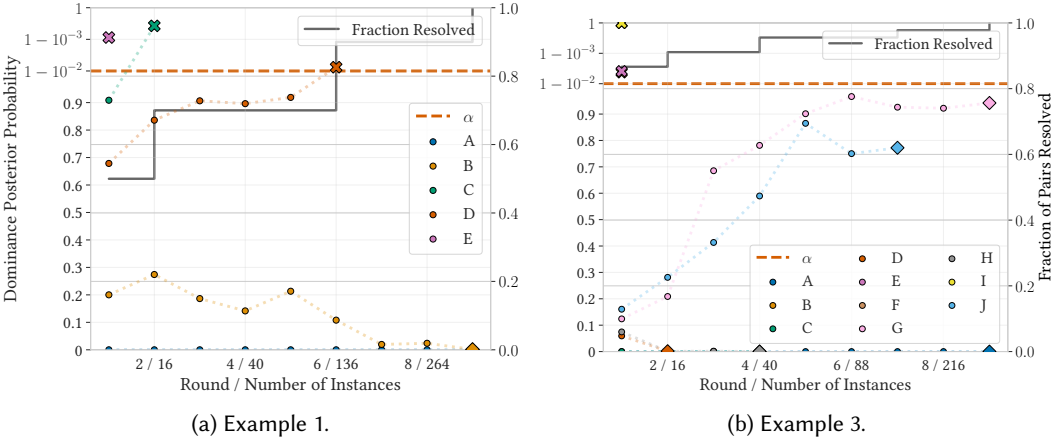


Fig. 3. Dominance posterior probabilities over rounds. Points show $\max_{A \in \mathcal{A}} P(A \succ^T B)$ for each algorithm B at each round (left y-axis). Note that the left y-axis changes to a log-scale for $p > 0.9$. A cross marks elimination, i.e., when the dominance probability climbs above the decision threshold α . A diamond marks that the algorithm is fully resolved and a Pareto set member. The black line shows the proportion of resolved algorithm pairs (right y-axis).

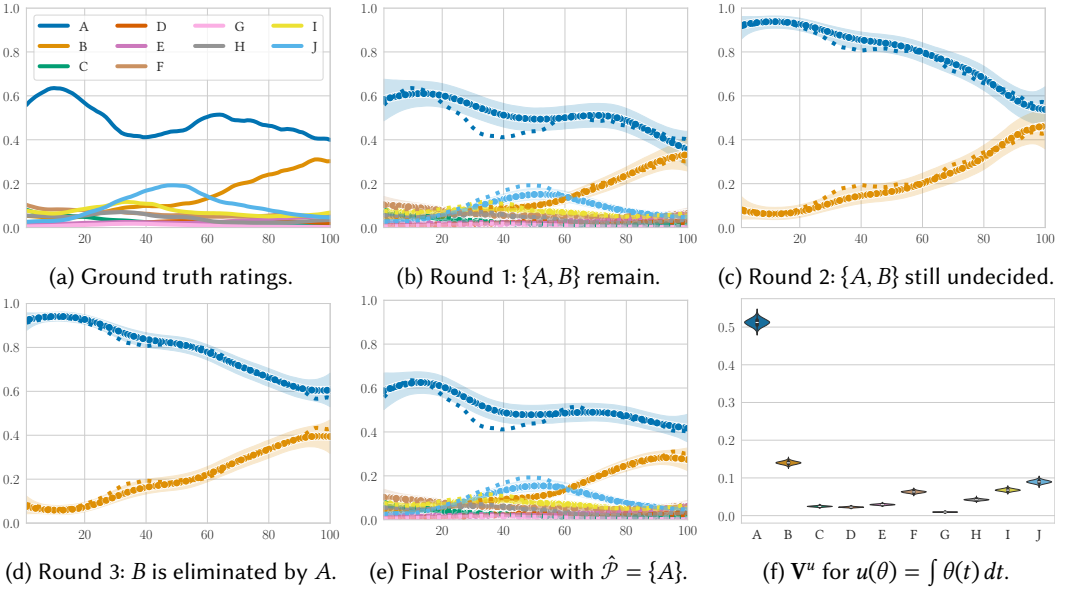


Fig. 4. A synthetic example with 10 algorithms. Conventions as in Figure 2.

$t > 14$, however not so close that the ROPE plays a role. It requires 6 rounds and a total of 136 instances to resolve that A dominates D . While B crosses A twice around $t = 14$, this is only by a little margin, and 9 rounds or 328 instances are necessary to be confident in this crossing, after which $\{A, B\}$ is correctly identified as the anytime Pareto set. Figure 2f shows the posterior over

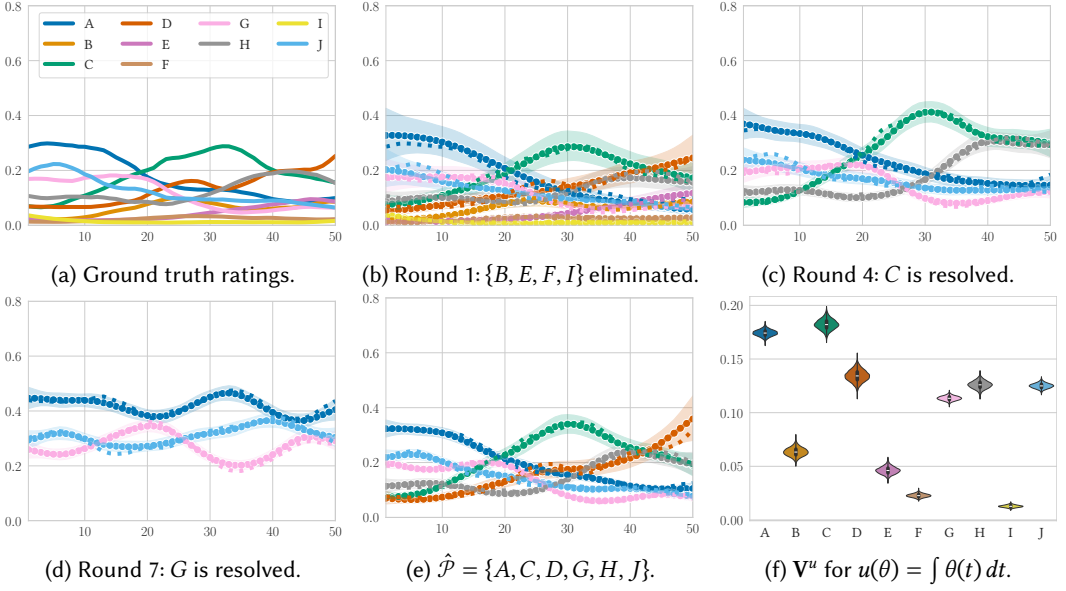


Fig. 5. A synthetic example with 10 algorithms. Conventions as in Figure 2. A resolved algorithm has all pairwise relationships determined; for non-eliminated algorithms, this confirms Pareto set membership.

preference values \mathbf{V}^u for a uniform preference $u(\theta) = \int \theta(t) dt$. This preference can also be understood as *noninformative*, i.e., we have no prior information about our budget, other than that it lies within t_1 and t_T . For this preference, A is the clear winner. Note that $\{C, D, E\}$ are included in this plot for illustrative purposes. Since they are anytime-dominated by A , they are worse for any strictly monotone preference, and must not be considered further. The evolution of the posterior over rounds is given in Figure 3a. Note how the number of sampled instances I on the x-axis increases irregularly with rounds due to batch size adaptation.

Example 2: Single Winner. The second example consists of 10 algorithms A to J , with $\mathcal{P} = \{A\}$, i.e., A dominates all other algorithms. The ground truth rating trajectories are given in Figure 4a. We use the HSGP model with $T = 100$. After the first round or 8 instances, all algorithms except B are eliminated by A . It takes a total of 3 rounds or 32 instances to assert that A and B do not cross for $t > 90$, and B is subsequently eliminated. Multiple rounds are expected here: A and B are similar at late timepoints, and the procedure correctly requires more evidence before eliminating. Figure 4f shows the posterior over V_u for the uniform preference, where A as the sole Pareto set member is naturally optimal.

Example 3: Near-Equivalence. The third example consists of 10 algorithms A to J , with $\mathcal{P} = \{A, C, D, H\}$. The ground truth rating trajectories are given in Figure 5a. We use the GP model with $T = 50$ and $M = 10$ inducing points. After the first round or 8 instances, $\{B, E, F, I\}$ are eliminated, some dominated by multiple algorithms. C is resolved early in the second round after 16 instances, since it confidently crosses all remaining Pareto set candidates. While G and J are dominated by A with respect to the ground truth, both fall within the ROPE relative to A at $t = 20$ and $t = 42$, respectively. As a consequence, G is resolved early after round 7 or 152 instances, and J follows after round 9 or 280 instances (cf. Figure 3b). Both are included in the final Pareto set $\hat{\mathcal{P}} = \{A, C, D, G, H, J\}$. This is a direct consequence of our choice of decision threshold $\alpha = 0.99$

together with equivalence threshold $\epsilon = 0.05$. The former encodes that we only eliminate when highly confident in dominance; the latter means that algorithms with pairwise win probability between 0.45 and 0.55 are considered practically interchangeable. Under preferences concentrated at $t = 20$ or $t = 42$, selecting G or J over A incurs negligible regret, and the distinction is not decision-relevant at the specified threshold. This example illustrates the tradeoff encoded by ϵ : larger values accept near-equivalent algorithms into the Pareto set, reducing sample cost but potentially including marginally inferior alternatives. Smaller values enforce stricter separation at higher sample cost. Nevertheless, the posterior over V_u confirms G and J as inferior compared to A under the uniform preference, with C being slightly more competitive than A under expectation (cf. Figure 5f).

5.2 Comparing Algorithms on Known Benchmarks (MA-BBOB)

The second case study applies POLARBEAR to a traditional benchmark setting, i.e., well-studied problem instances with known global optima. This enables direct comparison of assumptions and conclusions between POLARBEAR and established methods for anytime performance evaluation, such as EAF, ECDF, and AOCC. The goal is not to draw conclusions about the specific algorithms but to verify that POLARBEAR produces conclusions consistent with established methods, while requiring weaker assumptions and providing uncertainty quantification.

Setup. As an example of a typical benchmarking setup we compare seven algorithms: six modular CMA-ES variants [de Nobel et al. 2021] differing in step-size adaptation mechanism (CSA, MSR, TPA, XNES, MXNES, LPXNES) and random search (RS). Step-size adaptation is a core component of evolution strategies with substantial impact on convergence behavior, making these variants a natural test case with expected diversity in anytime behavior. All CMA-ES variants share a common baseline configuration, which is given in Section B. RS is included as a sanity-check baseline, which is generally good practice; here, it also anchors interpretation by providing a natural reference point against which practical usefulness can be judged.

Instances are drawn from MA-BBOB generator [Vermetten et al. 2023], which generates problems as affine combinations of the classical BBOB functions [Hansen et al. 2009]. Crucially, this generator always has the minimal objective value $f_{\text{opt}} = 0$ for each instance, enabling min-max normalization for EAF/ECDF/AOCC aggregation. We apply standard methodology: objective values of 1000 instances are min-max normalized per instance using the lower bound 10^{-8} and upper bound 10^2 , then aggregated. The budget axis is function evaluations, discretized to $T = 200$ log-spaced timepoints from 100 up to $2000 \cdot d$ evaluations, with dimension $d = 30$. For POLARBEAR, we use the independent Dirichlet model with Pathfinder inference, pointwise elimination, and strict resolution. We deliberately use such a fine grid to demonstrate scalability of the independent model with Pathfinder inference. This resolution far exceeds what is necessary for characterizing anytime behavior, i.e., $T \in [20 \dots 50]$ would suffice for most practical purposes, but illustrates that computational cost remains tractable even at high temporal resolution. Inference parallelizes across timepoints, completing in under two minutes for $P = 1000$ instances and $n = 7$ algorithms on a modern laptop CPU with 8 threads.

Discussion. The ECDF is given in Figure 6a. It can be observed that no algorithm dominates over all budgets. Specifically, MXNES seems to lead by a small margin for $t < 2000$, after which CSA takes first place until $t \approx 20\,000$. XNES wins for the remaining budget up to the final $t = 60\,000$. The rating posterior after strict resolution is given in Figure 9a. POLARBEAR has identified the Pareto set $\hat{\mathcal{P}} = \{\text{CSA}, \text{TPA}, \text{MXNES}, \text{XNES}\}$. Both RS and LPXNES are clearly inferior and eliminated in round 1 and 3 or after 8 and 24 instances (cf. Figure 8). MSR is eliminated in round 21 or 168 instances. Note that

the posterior is smooth over time despite temporal correlation not being explicitly modelled. ECDF and rating posterior show qualitative agreement: algorithms that appear superior in the ECDF have higher posterior win probabilities. However, the posterior is more conservative regarding crossing points. Where the ECDF suggests trajectories of CSA and XNES cross around $t = 15\,000$, the posterior places the crossing later around $t = 30\,000$ while reflecting uncertainty about the exact transition. The earlier crossing on the ECDF is most likely an artifact of its integration of the magnitude of improvement, which is however not reliable in general (cf. Section 2).

AOCC (Figure 6b) and value posterior of the uniform preference (Figure 9d) show similar trends (as expected since they derive from the ECDF and rating posterior), but differ in details. While AOCC slightly prefers XNES by mean (since the ECDF places the crossing earlier), the value posterior selects CSA under P2BB, expectation, and lower quantile risk profiles. However, XNES only loses by a tiny margin. The remaining ordering agrees, but AOCC only detects a small difference in mean between CSA and MSR, while the value posterior shows clear superiority of CSA under this preference. Figure 9c shows preference values for a log-uniform preference, weighting early performance much more heavily. Despite MXNES being optimal for $t < 1000$, CSA wins when taking the entire preference into account.

Crucially, the distributions of per-instance AOCC (and thus ECDF) values in Figure 6b reveal bimodality for most algorithms (except LPXNES and RS), with mass concentrated at both extremes. We attribute this to the log-transform in objective space, which clusters instances into “nearly solved” (high AOCC) and “far from solved” (low AOCC). This illustrates a fundamental limitation of AOCC as typically used: the mean over instances summarizes a bimodal distribution with a single number falling between the modes, where almost no actual instances lie. The implied “average performance” thus corresponds to no typical behavior. The ranking-based approach sidesteps this by estimating win probability, which is a quantity that remains interpretable regardless of the underlying performance distribution.

The EAF difference of selected algorithm pairs is given in Figure 7. The plots agree with POLARBEAR’s eliminations: MXNES dominates LPXNES and RS, while XNES dominates MSR. Between CSA and TPA, the latter only is better for a small range around $t < 1000$, which is consistent with the posterior (cf. Figure 9a). Notably, TPA never has the highest win probability at any individual timepoint, yet remains in the Pareto set because no single algorithm dominates it everywhere. This reflects the framework’s purpose: TPA is optimal under some strictly monotone preference, even if it never leads at any single moment. CSA and MXNES clearly do not dominate each other since MXNES is better earlier, and CSA is better later; the same is true for CSA versus XNES, where CSA is better earlier, and XNES is better later.

POLARBEAR took 59% less total function evaluations ($1.72 \cdot 10^8$ vs. $4.2 \cdot 10^8$ function evaluations) compared to evaluating all seven algorithms up to the maximal budget on 1000 instances, as standard practice for MA-BBOB [Vermetten et al. 2023]. Beyond eliminating dominated algorithms to save computational budget, the sampling strategy of pointwise elimination reduces effective function evaluations by skipping resolved late timepoints. Consequently, the posterior in Figure 9b shows higher uncertainty beyond the last crossings while still being confident about the respective relation. In total, POLARBEAR sampled 1656 different instances until full resolution of all pairs. The exact allocation of function evaluations and instances is given in Figure 10, which shows that CSA and XNES were only evaluated on 168 instances with more than half the total budget (i.e., $t > 32\,000$). In general, only Pareto set members were sampled on more than 1000 instances, necessitated by the strict resolution mode, which requires resolving all pairwise relationships to high certainty. Note that these savings are problem-dependent: they arise because several algorithms were clearly dominated and eliminated early, and because late timepoints could be resolved with comparatively few instances. Problems with more similar algorithms would require more samples,

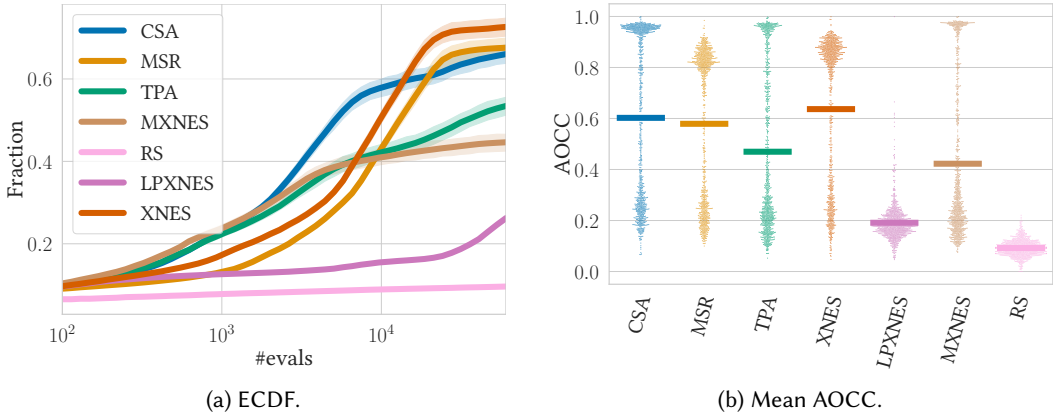


Fig. 6. ECDF (a) and AOCC (b) for the MA-BBOB case study, using 1000 instances. The ECDF shows the mean attained fraction of the interval $[10^{-8}, 10^2]$, scaled logarithmically. The shaded region is the 95% confidence interval of the mean, constructed by bootstrapping. The mean AOCC (dashes) is the area under the ECDF, using a linear x-axis. Points are the full AOCC distribution over instances.

which is entirely the point of allocating effort adaptively. Traditional methods lack such a principled stopping criterion and require exhaustive evaluation before analysis. POLARBEAR terminates when comparisons are resolved, concentrating effort exactly where it is needed.

This case study shows that traditional anytime analysis and POLARBEAR largely agree on which algorithms are competitive, validating the ranking-based approach against established methodology. However, POLARBEAR offers three advantages: uncertainty quantification, no assumptions about objective scale, and adaptive allocation of computational effort.

5.3 Comparing Algorithms under Arbitrary Instance Distributions (GP-BBOB)

The third case study demonstrates POLARBEAR on a setting where traditional anytime evaluation methods are not easily applicable: an arbitrary instance distribution with unknown global optima (or unknown objective scale in general) and highly heterogeneous dimensionality.

Setup. We compare eight algorithms: seven modular CMA-ES variants [de Nobel et al. 2021] differing in covariance matrix adaptation mechanism (cf. Table 2), and random search (RS) as a baseline. All CMA-ES variants share a common baseline configuration, which is given in Section B. Covariance matrix adaptation is the computational bottleneck of CMA-ES, with full adaptation scaling as $O(d^2)$ per generation and $O(d^3)$ for eigendecomposition. Cheaper approximations sacrifice adaptation quality for speed. The practical question for our hypothetical situation is: does expensive adaptation pay off in wall-clock time, particularly on the high-dimensional problems that are of interest for us?

Instances are drawn from GP-BBOB, a custom generator designed to simulate a deployment scenario where objective scale and global optima are unknown. GP-BBOB constructs problems as spatially-varying sparse mixtures of BBOB functions, producing nonstationary landscapes where the active problem components change across the search domain. Unlike MA-BBOB, global optima are not analytically recoverable. Dimensionality is drawn from $d \sim [\mathcal{N}(240, 30^2)]$, truncated to $[2, 320]$, reflecting heterogeneous problem scales. We make no claim that this distribution resembles any particular real-world application; it serves as an exemplary complex distribution to

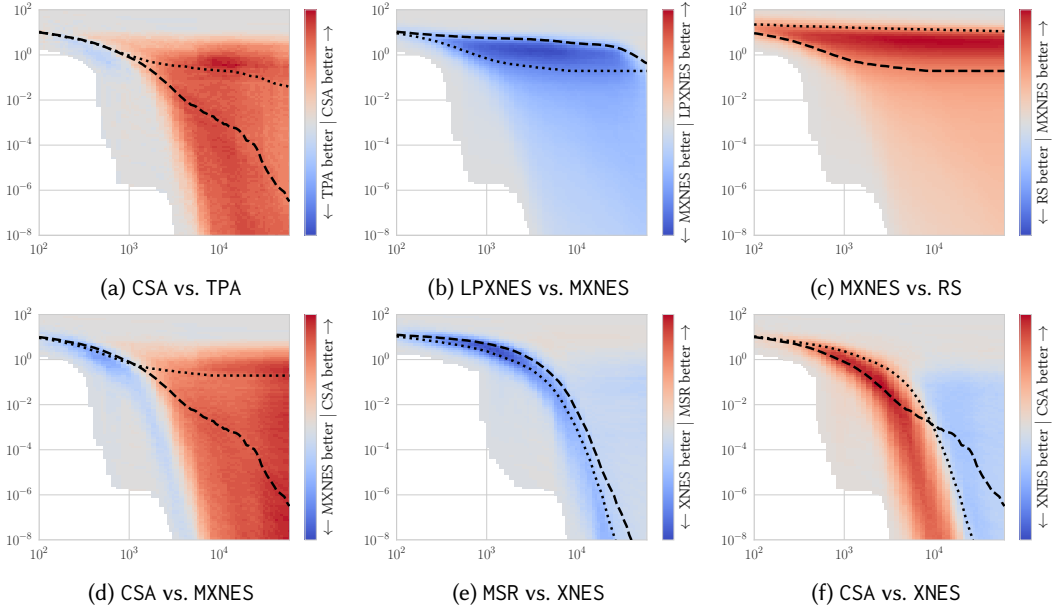


Fig. 7. EAF difference of selected algorithm pairs of the MA-BBOB case study on 1000 instances. In the EAF, color encodes the proportion of runs that attained at least the objective target $z - f_{\text{opt}}$ (y-axis) at a specific number of function evaluations (x-axis). Here, the difference of two such EAF surfaces is shown, with color encoding the difference in run proportions (red means first algorithm better, blue means second better, gray means no difference). The dashed line shows the median EAF contour (i.e., for each t , the $z - f_{\text{opt}}$ which 50% of runs have attained) of the first algorithm; dotted line shows the same of the second algorithm.

demonstrate that POLARBEAR operates where traditional methods struggle. Full details on the generator are given in Section C.

The budget axis is wall-clock time, discretized to $T = 30$ uniformly spaced timepoints from 0.1 to 30 seconds. This choice reflects practical deployment where actual computational cost, not only evaluation count, is the binding constraint. For POLARBEAR, we use the B-spline model with MCMC inference (4 chains; 1000 warmup samples, 2000 samples per chain), joint elimination, and crossing resolution.

Discussion. The posterior at key rounds is given in Figure 11, with Figure 12 showing the evolution of dominance posterior probabilities over rounds. A total of 14 rounds or 528 instances were necessary to identify the Pareto set $\hat{\mathcal{P}} = \{\text{NONE}, \text{SEP}\}$. This directly answers the motivating question: on this specific high-dimensional instance distribution under wall-clock budget, expensive covariance adaptation does *not* pay off. The $O(d^3)$ eigendecomposition cost of COV and the $O(d^2)$ alternatives (MAT, CHO, CMSA) are dominated by the $O(d)$ diagonal adaptation (SEP) and no adaptation (NONE). Notably, NAT is eliminated first, likely due to the computational cost of the matrix exponential. Under uniform time preference, NONE and SEP are nearly indistinguishable, with NONE winning by a small margin (Figure 11f). The choice between them depends on whether early or late budgets matter more: SEP should be preferred if the budget lies below 10 seconds, and NONE for longer budgets. This is detected by the crossing resolution, resolving this pair early and ending the race after CHO is eliminated in round 14.

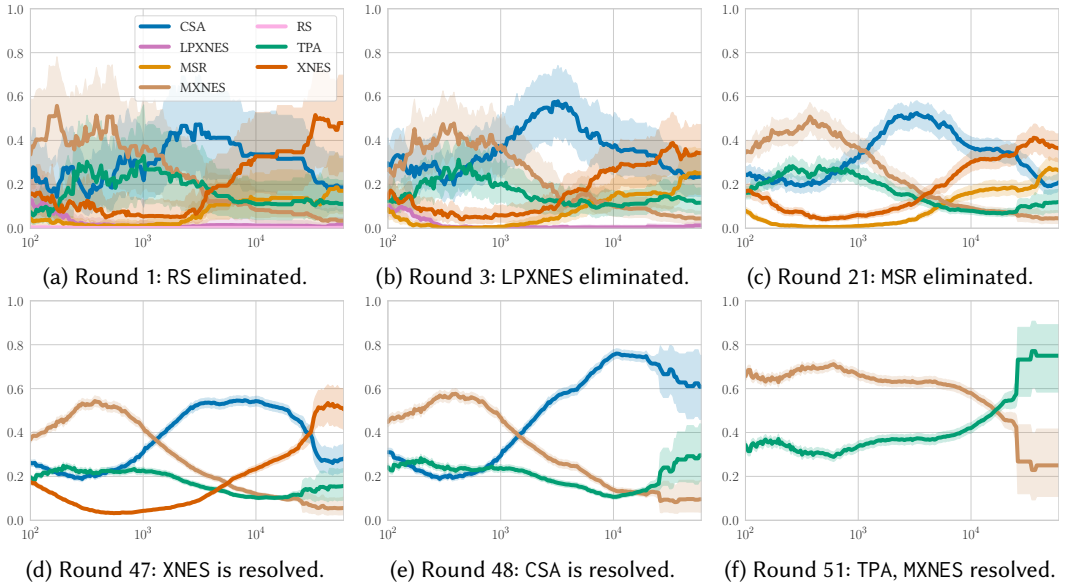


Fig. 8. Key POLARBEAR rounds for the MA-BBOB case study. The figures show the mean and 95% credible interval of the rating posterior (y-axis) over function evaluations (x-axis). A resolved algorithm has all pairwise relationships determined; for non-eliminated algorithms, this confirms Pareto set membership.

This finding, i.e., that cheap or no adaptation dominates on this particular high-dimensional instance distribution under wall-clock budget on our specific hardware, does not necessarily generalize to other distributions or hardware. But that is precisely the point: practitioners can now answer such questions for their specific conditions. Without POLARBEAR, answering this question would require substantial methodological compromise. Traditional anytime analysis requires known global optima for normalization, forcing practitioners to either construct artificial benchmarks with analytically tractable optima, sacrificing realism, or use observed minima as proxies, introducing instability as new algorithms shift the reference. Wall-clock time as budget axis is rarely used because it depends on hardware and implementation details that confound cross-study comparison. Heterogeneous dimensionality complicates aggregation further, as normalizing across instances of different scales conflates problem difficulty with dimensionality effects. Finally, all algorithms must be run to completion on all instances before analysis can begin, since there is no principled early stopping. POLARBEAR sidesteps these constraints: rankings require no normalization, any budget axis is valid, heterogeneous instances aggregate coherently, and adaptive sampling terminates when pairwise relationships are resolved. Rather than measuring on controlled benchmarks and hoping conclusions transfer, practitioners can measure the actual quantity of interest, such as wall-clock performance on the target instance distribution and deployment hardware.

6 Related Work

Our approach directly builds on the Bayesian ranking-model perspective introduced by Calvo et al. [2018, 2019], who advocate PL models as a principled way to transform repeated-run outcomes into probabilistic statements about algorithm orderings, including calibrated uncertainty and winning

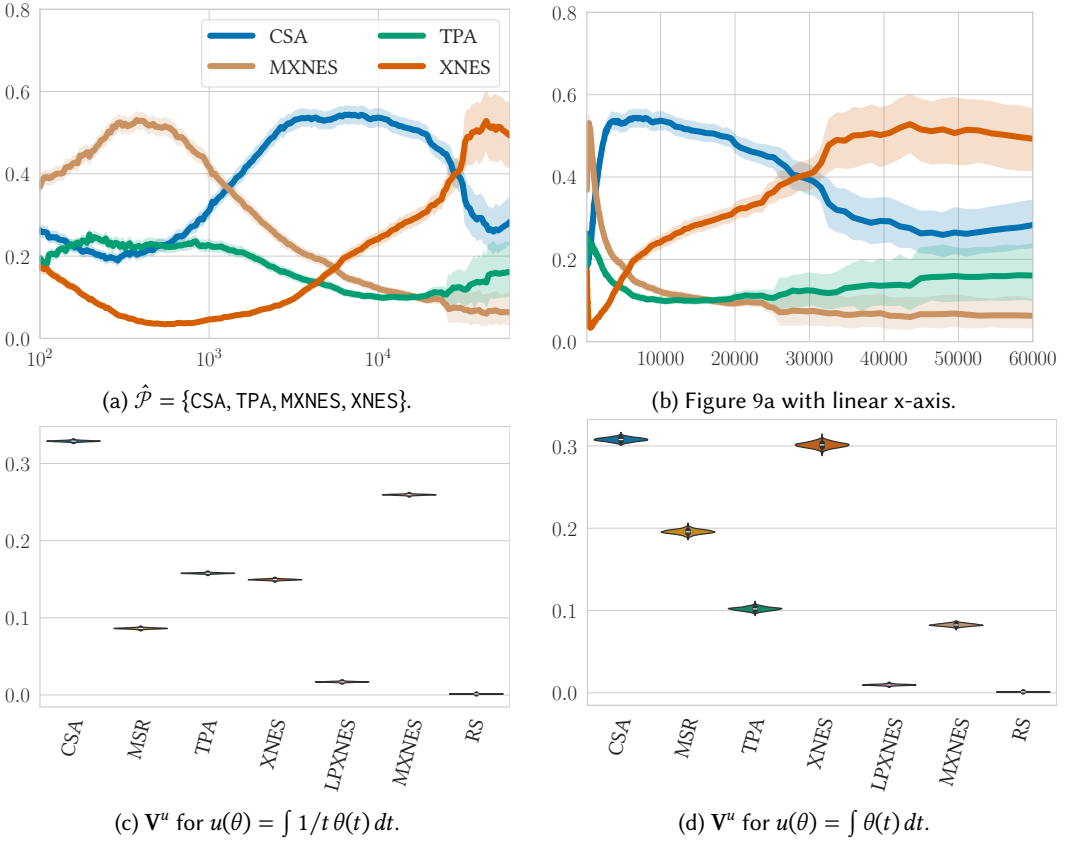


Fig. 9. Figure (a) and (b) show the mean and 95% credible interval of the final rating posterior of the anytime Pareto set for the MA-BBOB case study over function evaluations on a log and linear x-axis, respectively. Figure (c) and (d) show the resulting posterior over preference values for a uniform and log-uniform (i.e., $w(t) = 1/t$) budget preference, being the area under the curve of (a) and (b), respectively. Algorithms in the Pareto set are optimal under different time preferences; selection among them requires specifying such a preference at deployment.

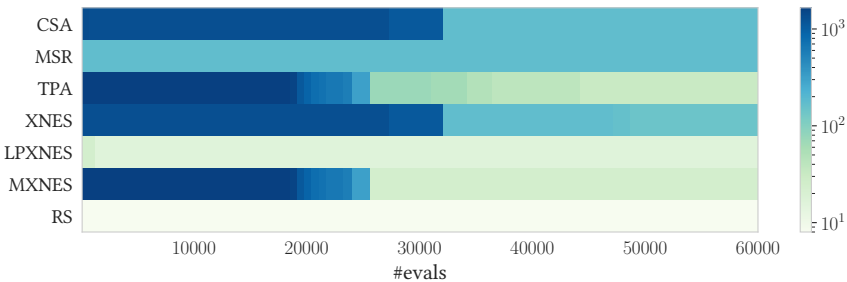


Fig. 10. Allocation of function evaluations and instances per algorithm by POLARBEAR for the MA-BBOB case study. Color shows the number of instances that saw the respective amount of function evaluations. Pointwise elimination allows reducing sample costs even for non-dominated algorithms by evaluating algorithms only up to their largest unresolved budget. This adaptive allocation achieves 59% fewer total function evaluations compared to the standard practice of running all algorithms to completion on 1000 instances.

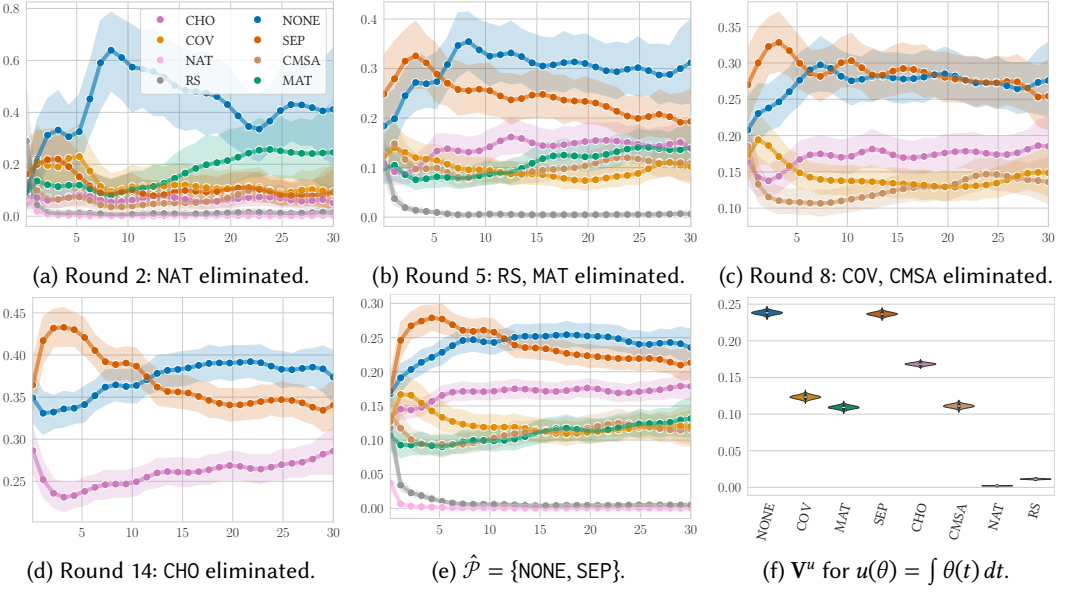


Fig. 11. Key POLARBEAR rounds and posteriors for the GP-BBOB case study. Figures (a) to (e) show the mean and 95% credible interval of the rating posterior (y-axis) over wall-clock time in seconds (x-axis). Figure (f) shows the resulting posterior over preference values for a uniform budget preference.

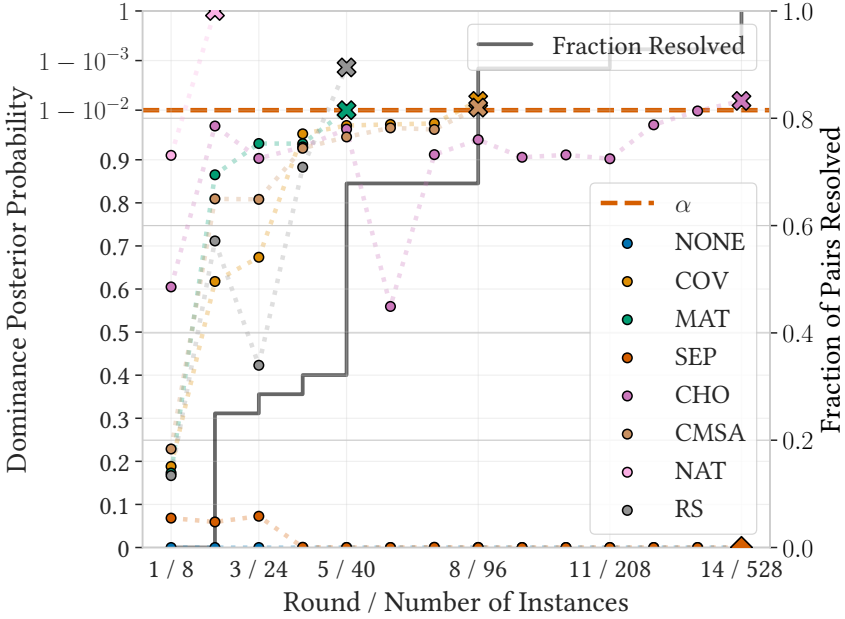


Fig. 12. Dominance posterior probabilities over rounds for the GP-BBOB case study. Conventions as in Figure 3. The drop in dominance posterior probability of CHO in round 6 can be attributed to high uncertainty whether it might cross NONE and SEP at 0.1s and 30s, respectively, given current observations (cf. Figure 11b).

Table 2. Modular CMA-ES variants compared in the GP-BBOB case study, differing in covariance matrix adaptation mechanism. Complexity is per-generation cost in dimension d .

Variant	Adaptation mechanism	Complexity
COV	Full covariance with eigendecomposition	$O(d^3)$
SEP	Diagonal only	$O(d)$
MAT	Direct transformation matrix (rank-one + rank- μ)	$O(d^2)$
CHO	Cholesky factor with rank updates	$O(d^2)$
CMSA	Exponential moving average + Cholesky recomputation	$O(d^2)$
NAT	Matrix exponential of natural gradient	$O(d^3)$
NONE	No matrix adaptation (step-size only)	$O(d)$

probabilities. Rojas-Delgado et al. [2022] further develop this view by emphasizing inference on relative orderings and expanding posterior summaries for algorithm comparison.

A close point of comparison is the work by Jesus et al. [2020], which also targets dynamic (deployment-time) interruption preferences, but solves it in a very different way. They model an anytime algorithm by an empirical performance profile over the time–quality plane, with quality being the best objective value obtained if the run is interrupted at a specific time. A decision maker specifies a utility density (known only at selection time), and the profile is reduced to a scalar score via a weighted volume. The algorithm maximizing this volume is selected for deployment, where the performance profile for a new instance is predicted by aggregating traces from similar training instances. Because the profile is defined over a common quality axis, this approach relies on normalization (in their case, relative hypervolume using best-known values) to make qualities comparable across instances.

Fawcett et al. [2023] derive statistically robust rankings from competition data via bootstrap resampling with Holm–Bonferroni correction. Rook et al. [2024] extend this idea to multi-objective assessment by replacing scalar scores with non-dominated sorting: each bootstrap replicate induces non-dominated layers, and solvers are robustly ranked based on their (replicate-wise) non-dominated ranks and dominance-based testing. Building on this line, Vermetten et al. [2025] apply robust ranking *over time* by repeating the (single- or multi-objective) robust ranking procedure at a sequence of fixed evaluation budgets, yielding a time series of snapshot rankings (with ties) that can change across budgets. A key limitation of budget-sliced robust ranking is that it yields a collection of budget-conditioned total preorders; interpreting anytime behavior then typically relies on comparing ranks across budgets. However, ranks (and rank differences) are inherently portfolio-dependent (i.e., violate IIA): adding or removing a solver can change all ranks even if the underlying pairwise relation between two solvers is unchanged. It therefore attributes meaning to budget-to-budget changes in portfolio-relative ranks.

Ravber et al. [2024] propose rating-based confidence bands for dynamic benchmarking: at each evaluation cutpoint t , algorithm runs are converted into win/loss/tie outcomes using error-to-known-optimum, and a Glicko-2 rating R_t with rating deviation RD_t is computed, yielding rating intervals $[R_t \pm 2RD_t]$; plotting these intervals over t provides an interpretable visualization of performance changes and a heuristic interpretation of significance across stages of execution via interval overlap. It is therefore fundamentally a sequence of budget-conditioned snapshot rankings (one tournament per cutpoint) rather than inference about anytime dominance.

Yan et al. [2022] analyze benchmarking paradoxes arising when conclusions change as solvers are added or removed. They trace this to algorithm-dependent success filters (e.g., defining success

relative to the best value in the pool) and propose algorithm-independent filters anchored to known optima or fixed targets. This achieves set-invariance but requires problem-side anchors. The PL model provides invariance through model structure: IIA guarantees that pairwise win probabilities are unaffected by the presence of other algorithms, without requiring known optima.

Campelo and Wanner [2020] provide a principled frequentist design algorithm comparison, including (1) instance-level repetition allocation that greedily reduces the worst standard error among paired comparisons until a target standard error is met, and (2) instance sample-size calculations that control family-wise error (e.g., via Holm) while achieving a desired power for detecting a minimally relevant effect size. Our methodology is similar in spirit in that it adaptively allocates evaluations until a worst-case stopping criterion is satisfied, but differs in the object of inference and stopping rule: rather than powering mean-difference tests at a fixed performance indicator, we terminate when pairwise relations are sufficiently resolved to support anytime dominance claims (including practical equivalence via a ROPE), which we interpret as minimizing worst-case regret over preference functionals. Moreover, we exploit temporal structure (e.g., early detection of crossings) and allow posterior-driven, user-specified early stopping criteria that are not captured by fixed- α /power design targets.

Eftimov and Korošec [2025] propose an online heuristic for choosing the number of repeated runs of a stochastic optimizer on a fixed instance. They incrementally add runs until the sample skewness (after centering by the sample mean and optionally removing outliers) lies within a preset band, treating approximate symmetry around the mean as an indicator that the collected runs are sufficiently representative. However, outcome distributions are often bounded, heavy-tailed, or mixture-like (e.g., rare very good runs), for which persistent skewness is expected. Symmetry is thus not directly tied to the decision-relevant uncertainty. Accordingly, our stopping criterion is formulated in terms of resolving pairwise relations to the desired posterior confidence, rather than enforcing a distribution-shape property of marginal outcomes.

Classical racing methods such as F-Race [Birattari et al. 2010] eliminate candidates online by evaluating all surviving candidates on a growing sequence of instances (a blocked design) and applying nonparametric tests on within-instance ranks; when a family-wise test detects differences, candidates significantly worse than the current best-ranked one are discarded and the race continues. Iterated racing, as implemented in *irace* [López-Ibáñez et al. 2016], wraps this idea in an outer loop that repeatedly samples new candidate configurations from an adaptive model and uses racing as a selection heuristic inside each iteration; importantly, the statistical tests are treated as heuristic filters rather than as calibrated sequential inference (e.g., *irace* explicitly avoids multiple-comparison corrections because they can prevent elimination). SPRINT-Race targets multi-objective model/solver selection by sequentially resolving pairwise dominance/non-dominance via a sequential probability ratio test with an indifference zone, and uses a Bonferroni argument to control the probability of erroneous eliminations over all pairwise tests in a fixed-confidence setting [Zhang et al. 2015]. At a high level, POLARBEAR is closest in spirit to fixed-confidence racing on a given instance distribution, but it differs in two ways that matter for anytime algorithm design. First, whereas F-Race/*irace* optimize a scalar objective (such as AOCC) and SPRINT-Race targets Pareto optimality in objective space, our comparison target is anytime dominance across budgets. Second, the rank-based blocked tests used in F-Race/*irace* are inherently portfolio-dependent: adding a new candidate can change historical ranks and thus the underlying test statistics, so “late entry” is not naturally compositional (even though manual mid-race injection has been explored) [Birattari et al. 2010]. By contrast, the IIA structure of the PL model makes candidate insertion at any point well-defined.

Multi-fidelity methods such as successive halving and Hyperband [Li et al. 2018] eliminate candidates based on partial evaluations, but rely on the assumption that low-fidelity performance predicts high-fidelity performance. When this assumption fails, as with crossing trajectories where one algorithm dominates early and another dominates late, such methods may incorrectly eliminate candidates. POLARBEAR makes no extrapolation assumption; anytime Pareto optimality explicitly preserves algorithms with different budget-dependent strengths.

7 Conclusion and Future Work

This paper introduced a Bayesian framework for identifying Pareto-optimal anytime optimization algorithms. The framework rests on three ideas: (1) treating each timepoint as a separate objective yields an anytime Pareto set that preserves tradeoffs over time, (2) using rankings rather than objective values enables coherent aggregation across heterogeneous instances without normalization, and (3) Bayesian inference with Plackett-Luce models provides calibrated uncertainty about algorithm performance. POLARBEAR instantiates this framework as an adaptive racing procedure, enabling automated evaluation. The IIA property of Plackett-Luce is central to its efficiency: dominated algorithms can be eliminated early without invalidating inference about survivors, and new algorithms can be added at any time without restarting the analysis. Termination occurs when all pairwise relations are resolved to a specified belief threshold, at which point the output Pareto set supports selection under arbitrary strictly monotonic time preferences and risk profiles. To our knowledge, this is the first approach to combine scale-free ranking models, anytime Pareto optimality, and sequential Bayesian experiment design. It removes assumptions required by traditional anytime evaluation (such as requiring optima, meaningful objective scales, and manual interpretation), and enables benchmarking under conditions that directly match deployment. The motivating question—*what should we compute offline to support selection under any budget information that may arise at deployment?*—therefore has a precise answer: the anytime Pareto set with calibrated posteriors. This set contains exactly the algorithms that could be optimal under some time preference, and the posterior supports principled selection under any such preference without additional experiments. Case studies demonstrate that POLARBEAR agrees qualitatively with traditional methods where both are applicable, while adaptively focusing computational effort exactly where needed (resulting in 59% fewer function evaluations in the MA-BBOB study), and enabling comparisons under conditions where traditional methods struggle. Inference may be slow for data with many ties or fine temporal grids, particularly for temporal models; however, these are computational rather than methodological limitations.

Several directions extend the framework presented here. The current approach marginalizes over instances by pooling rankings. When instance features are available or instance sets are small, hierarchical models can capture algorithm-instance interactions, i.e., a global rating with instance-specific offsets, or a process over the joint time-instance feature space. This would enable instance-conditional algorithm selection while retaining scale-free comparison.

Comparing multi-objective algorithms via indicators such as hypervolume reduces Pareto dominance to a total order but reintroduces domain knowledge (e.g., through a reference point). A scale-free alternative would model dominance relations directly: for each instance, observe whether the Pareto front produced by A dominates that of B , vice versa, or neither (as when fronts cover non-overlapping regions of the objective space). Aggregating these ternary outcomes across instances requires modeling a distribution over partial orders. While each observed instance yields a valid transitive relation, parametric families for such distributions are less developed than ranking models, and tractable analogs of Plackett-Luce with properties like IIA remain an open problem.

The IIA property enables adding algorithms to the race at any time without invalidating existing inference. This opens a natural integration with automated algorithm design, where a proposal

strategy (e.g., Bayesian optimization, evolutionary search, or LLM-based generation) suggests new configurations based on the current Pareto set, POLARBEAR evaluates them against existing candidates, and the loop continues until the Pareto set stabilizes or a budget is exhausted. This would enable fully automated algorithm design pipelines where the Pareto set emerges from an iterative generate-and-test process, with POLARBEAR providing the statistical backbone for principled comparison throughout.

References

- Oriol Abril-Pla, Virgile Andreani, Colin Carroll, Larry Dong, Christopher J. Fonnesbeck, Maxim Kochurov, Ravin Kumar, Junpeng Lao, Christian C. Luhmann, Osvaldo A. Martin, Michael Osthege, Ricardo Vieira, Thomas Wiecki, and Robert Zinkov. 2023. PyMC: A Modern, and Comprehensive Probabilistic Programming Framework in Python. *PeerJ Computer Science* 9 (Sept. 2023), e1516. doi:10.7717/peerj-cs.1516
- Mauro Birattari, Zhi Yuan, Prasanna Balaprakash, and Thomas Stützle. 2010. F-Race and Iterated F-Race: An Overview. In *Experimental Methods for the Analysis of Optimization Algorithms*, Thomas Bartz-Beielstein, Marco Chiarandini, Luís Paquete, and Mike Preuss (Eds.). Springer, Berlin, Heidelberg, 311–336.
- Ralph Allan Bradley and Milton E. Terry. 1952. Rank Analysis of Incomplete Block Designs: The Method of Paired Comparisons. *Biometrika* 39, 3-4 (Dec. 1952), 324–345. doi:10.1093/biomet/39.3-4.324
- Borja Calvo, Josu Ceberio, and Jose A. Lozano. 2018. Bayesian Inference for Algorithm Ranking Analysis. In *Proceedings of the Genetic and Evolutionary Computation Conference Companion (GECCO '18)*. Association for Computing Machinery, New York, NY, USA, 324–325. doi:10.1145/3205651.3205658
- Borja Calvo, Ofer M. Shir, Josu Ceberio, Carola Doerr, Hao Wang, Thomas Bäck, and Jose A. Lozano. 2019. Bayesian Performance Analysis for Black-Box Optimization Benchmarking. In *Proceedings of the Genetic and Evolutionary Computation Conference Companion (GECCO '19)*. Association for Computing Machinery, New York, NY, USA, 1789–1797. doi:10.1145/3319619.3326888
- Felipe Campelo and Elizabeth F. Wanner. 2020. Sample Size Calculations for the Experimental Comparison of Multiple Algorithms on Multiple Problem Instances. *Journal of Heuristics* 26, 6 (Dec. 2020), 851–883. doi:10.1007/s10732-020-09454-w
- Jacob de Nobel, Diederick Vermetten, Hao Wang, Carola Doerr, and Thomas Bäck. 2021. Tuning as a Means of Assessing the Benefits of New Ideas in Interplay with Existing Algorithmic Modules. In *Proceedings of the Genetic and Evolutionary Computation Conference Companion (GECCO '21)*. Association for Computing Machinery, New York, NY, USA, 1375–1384. doi:10.1145/3449726.3463167
- Tome Eftimov and Peter Korošec. 2025. Adaptive Estimation of the Number of Algorithm Runs in Stochastic Optimization. In *Proceedings of the Genetic and Evolutionary Computation Conference*. Association for Computing Machinery, New York, NY, USA, 719–727.
- Chris Fawcett, Mauro Vallati, Holger H. Hoos, and Alfonso E. Gerevini. 2023. Competitions in AI – Robustly Ranking Solvers Using Statistical Resampling. arXiv:2308.05062 [cs] doi:10.48550/arXiv.2308.05062
- Andrew Gelman, John B. Carlin, Hal S. Stern, and Donald B. Rubin. 1995. *Bayesian Data Analysis*. Chapman and Hall/CRC, New York. doi:10.1201/9780429258411
- Nikolaus Hansen. 2023. The CMA Evolution Strategy: A Tutorial. arXiv:1604.00772 [cs] doi:10.48550/arXiv.1604.00772
- Nikolaus Hansen, Steffen Finck, Raymond Ros, and Anne Auger. 2009. *Real-Parameter Black-Box Optimization Benchmarking 2009: Noiseless Functions Definitions*. Report. INRIA.
- Matthew D. Homan and Andrew Gelman. 2014. The No-U-turn Sampler: Adaptively Setting Path Lengths in Hamiltonian Monte Carlo. *J. Mach. Learn. Res.* 15, 1 (Jan. 2014), 1593–1623.
- Alexandre D. Jesus, Arnaud Liefoghe, Bilel Derbel, and Luís Paquete. 2020. Algorithm Selection of Anytime Algorithms. In *Proceedings of the 2020 Genetic and Evolutionary Computation Conference (GECCO '20)*. Association for Computing Machinery, New York, NY, USA, 850–858. doi:10.1145/3377930.3390185
- Pascal Kerschke, Holger H. Hoos, Frank Neumann, and Heike Trautmann. 2019. Automated Algorithm Selection: Survey and Perspectives. *Evolutionary Computation* 27, 1 (March 2019), 3–45. doi:10.1162/evco_a_00242
- John K. Kruschke. 2018. Rejecting or Accepting Parameter Values in Bayesian Estimation. *Advances in Methods and Practices in Psychological Science* 1, 2 (June 2018), 270–280. doi:10.1177/2515245918771304
- Alp Kucukelbir, Dustin Tran, Rajesh Ranganath, Andrew Gelman, and David M. Blei. 2017. Automatic Differentiation Variational Inference. *J. Mach. Learn. Res.* 18, 1 (Jan. 2017), 430–474.
- H. O. Lancaster. 1965. The Helmert Matrices. *The American Mathematical Monthly* 72, 1 (1965), 4–12. jstor:2312989 doi:10.2307/2312989
- Lisha Li, Kevin Jamieson, Giulia DeSalvo, Afshin Rostamizadeh, and Ameet Talwalkar. 2018. Hyperband: A Novel Bandit-Based Approach to Hyperparameter Optimization. *Journal of Machine Learning Research* 18, 185 (2018), 1–52.

- Manuel López-Ibáñez, Jérémie Dubois-Lacoste, Leslie Pérez Cáceres, Mauro Birattari, and Thomas Stützle. 2016. The Irace Package: Iterated Racing for Automatic Algorithm Configuration. *Operations Research Perspectives* 3 (Jan. 2016), 43–58. doi:10.1016/j.orp.2016.09.002
- Manuel López-Ibáñez and Thomas Stützle. 2014. Automatically Improving the Anytime Behaviour of Optimisation Algorithms. *European Journal of Operational Research* 235, 3 (June 2014), 569–582. doi:10.1016/j.ejor.2013.10.043
- Manuel López-Ibáñez, Diederick Vermetten, Johann Dreo, and Carola Doerr. 2024. Using the Empirical Attainment Function for Analyzing Single-Objective Black-Box Optimization Algorithms. *IEEE Transactions on Evolutionary Computation* (2024), 1–1. doi:10.1109/TEVC.2024.3462758
- R. Duncan Luce. 1979 c1959. *Individual Choice Behavior: A Theoretical Analysis*. Greenwood Press, Westport, Conn.
- Radford M. Neal. 2011. MCMC Using Hamiltonian Dynamics. In *Handbook of Markov Chain Monte Carlo*. Chapman and Hall/CRC.
- R. L. Plackett. 1975. The Analysis of Permutations. *Journal of the Royal Statistical Society. Series C (Applied Statistics)* 24, 2 (1975), 193–202. jstor:2346567 doi:10.2307/2346567
- Joaquin Quiñero-Candela and Carl Edward Rasmussen. 2005. A Unifying View of Sparse Approximate Gaussian Process Regression. *Journal of Machine Learning Research* 6, 65 (2005), 1939–1959.
- Carl Edward Rasmussen and Christopher K. I. Williams. 2005. *Gaussian Processes for Machine Learning*. The MIT Press. doi:10.7551/mitpress/3206.001.0001
- Miha Ravber, Marjan Mernik, Shih-Hsi Liu, Marko Šmid, and Matej Črepinšek. 2024. Confidence Bands Based on Rating Demonstrated on the CEC 2021 Competition Results. In *2024 IEEE Congress on Evolutionary Computation (CEC)*. 1–8. doi:10.1109/CEC60901.2024.10611955
- Gabriel Riutort-Mayol, Paul-Christian Bürkner, Michael R. Andersen, Arno Solin, and Aki Vehtari. 2022. Practical Hilbert Space Approximate Bayesian Gaussian Processes for Probabilistic Programming. *Statistics and Computing* 33, 1 (Dec. 2022), 17. doi:10.1007/s11222-022-10167-2
- Jairo Rojas-Delgado, Josu Ceberio, Borja Calvo, and Jose A. Lozano. 2022. Bayesian Performance Analysis for Algorithm Ranking Comparison. *IEEE Transactions on Evolutionary Computation* 26, 6 (Dec. 2022), 1281–1292. doi:10.1109/TEVC.2022.3208110
- Jeroen Rook, Holger H. Hoos, and Heike Trautmann. 2024. Multi-Objective Ranking Using Bootstrap Resampling. In *Proceedings of the Genetic and Evolutionary Computation Conference Companion (GECCO '24 Companion)*. Association for Computing Machinery, New York, NY, USA, 155–158. doi:10.1145/3638530.3654436
- Stan Development Team. 2026. Stan Modeling Language Users Guide and Reference Manual, Version 2.38.0.
- Luke Tierney and Joseph B. Kadane. 1986. Accurate Approximations for Posterior Moments and Marginal Densities. *J. Amer. Statist. Assoc.* 81, 393 (March 1986), 82–86. doi:10.1080/01621459.1986.10478240
- Heather L. Turner, Jacob van Etten, David Firth, and Ioannis Kosmidis. 2020. Modelling Rankings in R: The PlackettLuce Package. *Computational Statistics* 35, 3 (Sept. 2020), 1027–1057. doi:10.1007/s00180-020-00959-3
- Niki van Stein, Diederick Vermetten, Anna V. Kononova, and Thomas Bäck. 2024. Explainable Benchmarking for Iterative Optimization Heuristics. arXiv:2401.17842 [cs] doi:10.48550/arXiv.2401.17842
- Aki Vehtari, Andrew Gelman, Daniel Simpson, Bob Carpenter, and Paul-Christian Bürkner. 2021. Rank-Normalization, Folding, and Localization: An Improved $R^{\hat{}}$ for Assessing Convergence of MCMC (with Discussion). *Bayesian Analysis* 16, 2 (June 2021), 667–718. doi:10.1214/20-BA1221
- Diederick Vermetten, Jeroen Rook, Oliver L. Preuß, Jacob de Nobel, Carola Doerr, Manuel López-Ibáñez, Heike Trautmann, and Thomas Bäck. 2025. MO-IOHinspector: Anytime Benchmarking of Multi-objective Algorithms Using IOHprofiler. In *Evolutionary Multi-Criterion Optimization*, Hemant Singh, Tapabrata Ray, Joshua Knowles, Xiaodong Li, Juergen Branke, Bing Wang, and Akira Oyama (Eds.). Springer Nature, Singapore, 242–256. doi:10.1007/978-981-96-3506-1_17
- Diederick Vermetten, Hao Wang, Manuel López-Ibáñez, Carola Doerr, and Thomas Bäck. 2022. Analyzing the Impact of Undersampling on the Benchmarking and Configuration of Evolutionary Algorithms. In *Proceedings of the Genetic and Evolutionary Computation Conference (GECCO '22)*. Association for Computing Machinery, New York, NY, USA, 867–875. doi:10.1145/3512290.3528799
- Diederick Vermetten, Furong Ye, Thomas Bäck, and Carola Doerr. 2023. MA-BBOB: Many-Affine Combinations of BBOB Functions for Evaluating AutoML Approaches in Noiseless Numerical Black-Box Optimization Contexts. In *Proceedings of the Second International Conference on Automated Machine Learning*. PMLR, 7/1–14.
- Yuan Yan, Qunfeng Liu, Li, and Yun. 2022. Paradox-Free Analysis for Comparing the Performance of Optimization Algorithms. *IEEE Transactions on Evolutionary Computation* (2022), 1–1. doi:10.1109/tevc.2022.3199647
- Furong Ye, Carola Doerr, Hao Wang, and Thomas Bäck. 2022. Automated Configuration of Genetic Algorithms by Tuning for Anytime Performance. *IEEE Transactions on Evolutionary Computation* 26, 6 (Dec. 2022), 1526–1538. doi:10.1109/tevc.2022.3159087
- Lu Zhang, Bob Carpenter, Andrew Gelman, and Aki Vehtari. 2022. Pathfinder: Parallel Quasi-Newton Variational Inference. *Journal of Machine Learning Research* 23, 306 (2022), 1–49.

Tiantian Zhang, Michael Georgiopoulos, and Georgios C. Anagnostopoulos. 2015. SPRINT Multi-Objective Model Racing. In *Proceedings of the 2015 Annual Conference on Genetic and Evolutionary Computation (GECCO '15)*. Association for Computing Machinery, New York, NY, USA, 1383–1390. doi:10.1145/2739480.2754791

A Helmert Transformation

The Helmert matrix $Q \in \mathbb{R}^{n \times (n-1)}$ is an orthogonal contrast matrix used to parameterize the $(n-1)$ -dimensional subspace $\{x \in \mathbb{R}^n : \sum_{i=1}^n x_i = 0\}$ [Lancaster 1965]. The (i, k) -th entry for $k = 1, \dots, n-1$ is defined as:

$$Q_{i,k} = \begin{cases} \sqrt{\frac{1}{k(k+1)}} & \text{if } i \leq k \\ -\sqrt{\frac{k}{k+1}} & \text{if } i = k + 1 \\ 0 & \text{if } i > k + 1 \end{cases} \quad (38)$$

It has the following properties:

- Orthonormality: $Q^T Q = I_{n-1}$ where I_{n-1} is the identity matrix.
- Sum-to-zero: For any $\eta \in \mathbb{R}^{n-1}$, we have $\sum_{i=1}^n [Q\eta]_i = 0$.

In the context of Plackett-Luce models, the Helmert transformation ensures identifiability by constraining log-utilities to sum to zero, since adding a constant to all log-utilities does not change the ranking probabilities under the softmax transformation.

B CMA-ES Configuration

All modular CMA-ES variants use the following baseline configuration:

- Initial step size σ_0 : 2/10 of search space domain
- active: True
- repelling_restart: True
- threshold_convergence: False
- bound_correction: COTN
- restart_strategy: IPOP
- center_placement: UNIFORM

Case study 2 (MA-BBOB) fixes `matrix_adaptation=COV` and varies step-size adaptation. Case study 3 (GP-BBOB) fixes `ssa=CSA` and varies matrix adaptation.

These choices ensure budget-agnostic behavior: IPOP (rather than e.g., BIPOP) avoids budget-dependent restart scheduling, and disabling threshold convergence prevents early termination based on progress heuristics. As discussed in Section 2, budget-dependent configurations define algorithm families rather than single anytime algorithms; we avoid this complication by using configurations whose trajectories are independent of any configured budget.

C GP-BBOB: Input-Dependent Sparse Mixtures of BBOB Functions

GP-BBOB extends MA-BBOB [Vermetten et al. 2023] by making the mixture weights depend on the decision vector x . Let $\{f_i\}_{i=1}^{24}$ denote the BBOB base functions with fixed instances (here from the SBOX variant, i.e., optima are uniformly within the entire domain per function). The benchmark objective is defined as

$$f(x) = \sum_{i=1}^{24} w_i(x) f_i(x) + y_0, \quad (39)$$

where y_0 is an optional offset and $w(x) \in \Delta^{24}$ is an input-dependent weight vector.

We draw a latent logit field $z(x) \in \mathbb{R}^{24}$ from a (stationary) Gaussian process prior (implemented via random Fourier features):

$$z_i(x) \sim \mathcal{GP}(0, k_\ell(\cdot, \cdot)), \quad i = 1, \dots, 24, \quad (40)$$

where k_ℓ is an RBF kernel with lengthscale ℓ (and an amplitude σ). Given logits $z(x)$ and a temperature $T > 0$, we compute a sparse weight vector by restricting to the top- $k(x)$ indices,

$$S(x) = \text{TopK}(z(x), k(x)), \quad (41)$$

$$w_i(x) = \begin{cases} \frac{\exp(z_i(x)/T)}{\sum_{j \in S(x)} \exp(z_j(x)/T)}, & i \in S(x), \\ 0, & i \notin S(x). \end{cases} \quad (42)$$

Thus, at each x , only $k(x)$ base functions contribute.

The sparsity level $k(x) \in \{1, \dots, 24\}$ is itself input-dependent. We draw an independent scalar GP field $h(x)$ (again via random Fourier features),

$$h(x) \sim \mathcal{GP}(0, k_{\ell_k}(\cdot, \cdot)), \quad (43)$$

map it to a uniform random field using the Gaussian CDF Φ ,

$$u(x) = \Phi(h(x)) \in (0, 1), \quad (44)$$

and transform $u(x)$ to an integer via a discrete prior K chosen to roughly match the MA-BBOB sparsity distribution:

$$k(x) = F_K^{-1}(u(x)), \quad (45)$$

where F_K is the CDF of K on $\{1, \dots, 24\}$.

Unlike MA-BBOB (constant weights), the active set $S(x)$ changes across the domain, yielding a nonstationary, piecewise-smooth landscape. Consequently, the global minimizer is generally not analytically recoverable from the mixture construction. This is acceptable for our intended use as a hypothetical complex instance distribution where no domain knowledge is available. The parameters are itself sampled from priors, the exact definitions of which are given in Table 3. However, we emphasize that these were chosen ad-hoc, the only intention being that instances still have identifiable structure. Figure 13 shows an exemplary instance with $d = 2$. The resulting landscape shows the piecewise structure arising from position-dependent weights.

Table 3. Priors used for GP-BBOB in the third case study. Here $\text{LN}(\mu, \sigma)$ denotes a LogNormal distribution with underlying normal parameters, $\text{DU}\{a, \dots, b\}$ a discrete uniform distribution on integers, and $\text{Trunc}(\cdot; [a, b])$ truncation (not clipping) to the interval $[a, b]$.

Parameter	Prior	Notes / support
d (dimension)	$\text{Trunc}(\mathcal{N}(240, 30); [2, 320])$	integer cast
y_0 (offset)	$1000 \cdot \text{Cauchy}(0, 1)$	scalar
\mathbf{i} (instances)	$\text{UnifInt}\{1, \dots, 999\}^{24}$	i.i.d. per base function
T (logits temperature)	$\text{LN}(-0.5, 0.5)$	$T > 0$
m (RFF features for logits GP)	$\text{DU}\{32, \dots, 128\}$	integer cast
ℓ (logits GP lengthscale)	$\text{LN}(2.0, 1.0)$	$\ell > 0$
σ (logits GP amplitude)	$\text{LN}(0.0, 0.7)$	$\sigma > 0$
F_K (marginal for $k(x)$)	$\text{Trunc}(\text{LN}(1.1, 0.5); [2, 24])$	used as F_K^{-1}
m_k (RFF features for $k(x)$ GP)	$\text{DU}\{16, \dots, 64\}$	integer cast
ℓ_k ($k(x)$ GP lengthscale)	$\text{LN}(0.0, 1.0)$	$\ell_k > 0$
σ_k ($k(x)$ GP amplitude)	$\text{LN}(0.0, 0.7)$	$\sigma_k > 0$

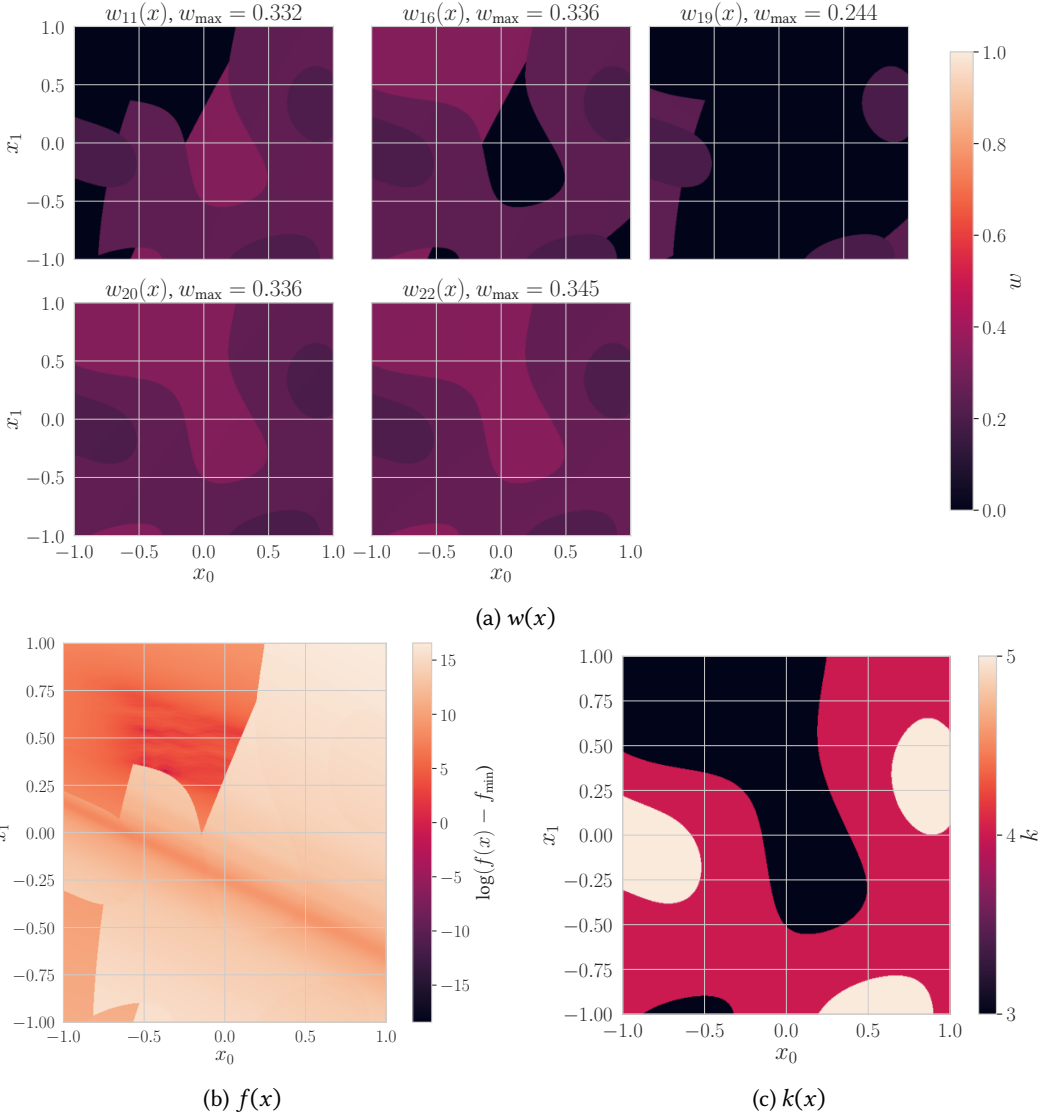


Fig. 13. A GP-BBOB instance with $d = 2$. Figure (a) shows $w(x)$ for all instances with any $w(x) > 0.001$. Figure (b) shows the sparsity level $k(x)$, and (c) shows the resulting landscape $f(x)$ with minimal observed value f_{\min} (from the plotting grid, not necessarily the global optimum) subtracted, then log-scaled.